BRNO UNIVERSITY OF TECHNOLOGY
VYSOKÉ UČENÍ TECHNICKÉ V BRNĚ

FACULTY OF CHEMISTRY
FAKULTA CHEMICKÁ

INSTITUTE OF CHEMISTRY AND TECHNOLOGY OF ENVIRONMENTAL PROTECTION
ÚSTAV CHEMIE A TECHNOLOGIE OCHRANY ŽIVOTNÍHO PROSTŘEDÍ

EXPLORING CORRELATION BETWEEN VEGETATION INDICES AND PLANT NITROGEN UPTAKE

PRŮZKUM KORELACE MEZI VEGETAČNÍMI INDEXY A PŘÍJMEM DUSÍKU ROSTLINAMI

BACHELOR'S THESIS
BAKALÁŘSKÁ PRÁCE

AUTHOR **ALENA PAVLAČKOVÁ**
AUTOR PRÁCE

SUPERVISOR **prof. Ing. JIŘÍ KUČERÍK, Ph.D.**
VEDOUCÍ PRÁCE

BRNO 2024

BRNO UNIVERSITY OF TECHNOLOGY
FACULTY OF CHEMISTRY

Assignment Bachelor's Thesis

Project no.:	FCH-BAK1959/2023	Academic year: 2023/24
Department:	Institute of Chemistry and Technology of Environmental Protection	
Student:	**Alena Pavlačková**	
Study programme:	Environmental Chemistry, Safety and Management	
Field of study:	no specialisation	
Head of thesis:	**prof. Ing. Jiří Kučerík, Ph.D.**	

Title of Bachelor's Thesis:

Exploring correlation between vegetation indices and plant nitrogen uptake

Bachelor's Thesis:

1. Literature review on nitrogen cycle, plant nitrogen uptake and vegetation indices.
2. Collection of biomass samples and analysis of nitrogen content. Obtaining values of vegetation indices from sampling areas using Google Earth Engine.
3. Elaboration of data in R studio and creating scatterplots; creation of linear models for prediction of nitrogen uptake and their verification.
4. Summarizing and discussing obtained data.

Deadline for Bachelor's Thesis delivery: 20.5.2024:

Bachelor's Thesis should be submitted to the institute's secretariat in a number of copies as set by the dean This specification is part of Bachelor's Thesis

Alena Pavlačková student	prof. Ing. Jiří Kučerík, Ph.D. Head of thesis	prof. Ing. Jozef Krajčovič, Ph.D. Head of department

In Brno dated 1.2.2024

prof. Ing. Michal Veselý, CSc.
Dean

Abstract

Excessive fertilization can cause environmental pollution, such as water contamination and greenhouse gas emissions, along with economic losses. To mitigate these issues, it is important to adjust fertilization rates to the specific needs of crops. This thesis explores the use of remotely sensed vegetation indices to monitor crop nitrogen uptake and guide fertilization application. The study was conducted in Oensingen, Switzerland, during an internship at ETH Zürich. The main objective was to develop a prediction model based on vegetation indices to estimate the nitrogen uptake of grass-clover mixtures and winter wheat. Additionally, the correlation between various vegetation indices and crop characteristics, especially nitrogen uptake, was analyzed. Vegetation indices (NDVI, NDRE, GNDVI, MCARI, EVI) were derived from Sentinel-2 images using Google Earth Engine. Various crop characteristics, including the Leaf Area Index (LAI) and crop height, were measured, and winter wheat samples were analyzed for nitrogen uptake using an elemental analyzer. Additional nitrogen uptake data for grass from previous years was also included. In total, data from the years 2021-2023, that included both grass-clover mixture and winter wheat values, were used in the analysis. Correlation and regression analysis were performed to examine the relationships between vegetation indices and the measured crop characteristics. The index showing the strongest relationship with crop nitrogen uptake was then used to create a prediction model. The analysis revealed that the Enhanced Vegetation Index (EVI) was the most effective predictor of nitrogen uptake. The constructed prediction model based on EVI values achieved a high coefficient of determination (R^2) of 0.89, a low root mean square error (RMSE) of 1.05, and a mean absolute error (MAE) of 0.89. The results indicate that EVI is a reliable index for predicting nitrogen uptake in crops. The developed EVI-based model could be potentially used for optimizing nitrogen application in crops, which can reduce the negative environmental and economic impacts of over-fertilization.

Abstrakt

Nadměrné hnojení může způsobit znečištění životního prostředí, jako je kontaminace vody a emise skleníkových plynů, a také ekonomické ztráty. Ke zmírnění těchto problémů je důležité přizpůsobit míru hnojení specifickým potřebám plodin. Ve své práci se zabývám možností využití dálkově snímaných vegetačních indexů pro monitorování příjmu dusíku rostlinami a řízení aplikace hnojiv. Měření byla provedena v Oensingenu, Švýcarsku, během stáže na ETH Zürich. Hlavním cílem bylo vyvinout predikční model založený na vegetačních indexech k odhadu příjmu dusíku travní směsi a ozimé pšenice. Dále byla analyzována korelace mezi různými vegetačními indexy a charakteristikami plodin, především příjmu dusíku. Vegetační indexy (NDVI, NDRE, GNDVI, MCARI, EVI) byly získány ze snímků družice Sentinel-2 pomocí Google Earth Engine. Byly změřeny různé charakteristiky plodin, včetně indexu listové plochy (LAI) a výšky plodin, a vzorky ozimé pšenice byly analyzovány na příjem dusíku pomocí elementárního analyzátoru. Do analýzy byla také zahrnuta další data týkající se příjmu dusíku travin z předchozích let. Celkem byla v analýze použita data z let 2021–2023, která zahrnovala hodnoty pro travní směs i ozimou pšenici. Byly provedeny korelační a regresní analýzy k určení vztahů mezi vegetačními indexy a měřenými charakteristikami plodin. Index, který vykazoval nejsilnější vztah s příjmem dusíku plodin, byl poté využit k vytvoření predikčního modelu. Analýza ukázala, že Enhanced Vegetation Index (EVI) byl nejúčinnějším prediktorem příjmu dusíku. Vytvořený predikční model založený na hodnotách EVI dosáhl vysokého koeficientu determinace (R^2) 0,89, nízké směrodatné odchylky chyb (RMSE) 1,05 a průměrné absolutní odchylky (MAE) 0,89. Výsledky naznačují, že EVI je spolehlivým indexem pro predikci příjmu dusíku plodinami. Vyvinutý model založený na EVI by mohl být potenciálně použit k optimalizaci aplikace dusíkatých hnojiv na plodiny, což by pomohlo snížit negativní environmentální a ekonomické dopady nadměrného hnojení.

Keywords

nitrogen cycle, nitrogen uptake, winter wheat, correlation, regression analysis, prediction modelling, spectral vegetation indices, remote sensing, precision agriculture, Sentinel-2, Leaf Area Index, LAI, Normalized Difference Vegetation Index, NDVI, atmospheric correction

Klíčová slova

cyklus dusíku, příjem dusíku, pšenice ozimá, korelace, regresní analýza, predikční modelování, spektrální vegetační indexy, dálkový průzkum Země, precizní zemědělství, Sentinel-2, index listové plochy, LAI, normalizovaný diferenční vegetační index, NDVI, atmosférická korekce

Reference

PAVLAČKOVÁ, Alena. *Exploring correlation between vegetation indices and plant nitrogen uptake*. Brno, 2024. Bachelor's thesis. Brno University of Technology, Faculty of Chemistry. Supervisor prof. Ing. Jiří Kučerík, Ph.D.

Exploring correlation between vegetation indices and plant nitrogen uptake

Declaration

I declare that the bachelor thesis has been worked out by myself and that all the quotations from the used literary sources are accurate and complete. The content of the bachelor thesis is the property of the Faculty of Chemistry of the Brno University of Technology, and all commercial uses are allowed only if approved by both the supervisor and the Dean of the Faculty of Chemistry BUT.

.....
Alena Pavlačková
May 19, 2024

Acknowledgements

I would like to express my gratitude to my supervisor prof. Ing. Jiří Kučerík, PhD., for his support and professional guidance in writing the thesis. I extend my profound gratitude to prof. Dr. Nina Buchmann for giving me the opportunity to carry out this work at the Grassland Sciences group at ETH Zürich. I am greatly thankful to Fabio Turco who suggested the thesis topic and guided me through the data acquisition. I also thank everyone else at ETH Zürich who provided me with data used in this work and/or helped me with the measurements and gave me advice. Last but not least, I am greatful for the support of my boyfriend and my family.

Contents

List of Figures

List of abbreviations

anammox anaerobic ammonium oxidation.

EVI Enhanced Vegetation Index.

GEE Google Earth Engine.

GNDVI Green Normalized Difference Vegetation Index.

LAI Leaf Area Index.

LOOCV Leave-One-Out Cross-Validation.

MAE Mean Absolute Error.

MCARI Modified Chlorophyll Absorption in Reflectance Index.

NDRE Normalized Difference Red Edge.

NDVI Normalized Difference Vegetation Index.

NIR Near-Infrared.

PA Precision Agriculture.

RMSE Root Mean Square Error.

VI Vegetation Index.

1 Introduction

Nitrogen plays a crucial role in supporting plant growth, influencing factors such as yield, quality, and overall crop health. To ensure that plants receive the necessary amount of nitrogen, it is introduced into the soil through the application of either synthetic or natural N-fertilizers. Synthetic fertilizers are produced in the Haber-Bosch process, which was developed in the early 20th century by the German chemists Fritz Haber and Carl Bosch. In this catalytic process, molecular nitrogen is converted to ammonia under high temperature and pressure conditions, which is then used for fertilizer production [1]. The use of nitrogen fertilizers on an industrial scale was made possible through this groundbreaking process and has significantly boosted agricultural productivity, playing an important role in sustaining the nutritional needs of the growing global population.

However, excessive nitrogen application often leads to the accumulation of this nutrient in the soil, since crops typically use only around 50% or less fertilizer nitrogen added to the soil [2]. The rest is lost to the environment through various pathways or remains in the soil. This accumulation often leads to various environmental problems. Excess nitrogen can alter the pH balance of the soil, leading to soil acidification or alkalization. This disruption in pH results in changes in the structure of the soil, reducing its ability to hold water and nutrients. Furthermore, high levels of nitrogen modify the composition of the microbial community, favoring species that thrive in nutrient rich environments while suppressing others [3]. This reduced microbial diversity can compromise important soil processes such as organic matter decomposition and nitrogen fixation. When combined with excessive irrigation or heavy rain, nitrogen in the soil also contributes to the release of N_2O, a potent greenhouse gas. Agriculture contributes significantly to these emissions, accounting for approximately 80% of the total N_2O emissions [4]. In addition, excessive nitrogen accumulation can result in nitrate leaching, a process in which nitrates move through the soil profile and infiltrate groundwater, posing potential risks to human health. Therefore, it is crucial to optimize fertilizer use efficiency to prevent nitrogen accumulation in the soil. Fertilizer use efficiency is defined as the ratio between nutrients absorbed by plants and the amount of fertilizer applied [5]. Enhancing fertilizer use efficiency can be achieved by tailoring fertilizer rates to local and current crop needs [6], an approach known as precision nitrogen management [7]. This strategy not only reduces the environmental impacts of excessive nitrogen application, but is also economically beneficial, considering the high cost of fertilizers.

Monitoring nitrogen uptake is crucial for adjusting fertilizer rates and determining the specific nitrogen needs of crops. Conventionally, nitrogen uptake has been measured using manual and destructive methods, where crop samples are obtained from the field and subsequently analyzed in the laboratory. However, such techniques are time-consuming and associated with other significant drawbacks, including high costs, labor-intensive procedures, and limited representation of spatial or temporal variability. To overcome these limitations, satellite-derived vegetation indices have emerged as a potential alternative to monitor nitrogen uptake in crops [8]. Unlike traditional methods, satellite-derived vegetation indices provide more efficient and cost-effective means of monitoring nitrogen uptake in crops.

In this thesis, the correlation between remotely sensed vegetation indices and crop nitrogen uptake was analyzed. The goal was to explore the possibility of using these indices to adjust fertilizer rates and reduce the negative impact of agriculture on the environment. Although these indices can provide field-scale crop information quickly and easily, they provide less accurate results. Nevertheless, the utilization of satellite-derived vegetation indices holds the promise of enabling remote near-real-time measurement of crop nitrogen uptake, offering considerable advantages over current methodologies in practice.

2 State of the art

This chapter presents the theoretical background of the thesis topic. First, it describes the nitrogen cycle and how it is disrupted by anthropogenic activities, along with the resulting consequences. Next, the principles of precision agriculture and remote sensing are introduced, and the use of satellite imagery to monitor and manage crops is explained. Lastly, the chapter contains a description of vegetation indices used in the analysis and references similar research to provide context.

2.1 Nitrogen cycle

Nitrogen is an essential component of proteins, DNA, and chlorophyll, which makes it vital for all living organisms, including plants. Nitrogen compounds can be divided into two categories: non-reactive and reactive. Dinitrogen (N_2) is non-reactive due to its strong triple bond, which most organisms are unable to break. On the other hand, reactive nitrogen (Nr) refers to nitrogen compounds that are chemically active or readily available for biological and chemical processes [9]. Although N_2 gas is abundant in the atmosphere, plants cannot directly utilize it due to its inert nature. It must first be converted into a reactive nitrogen compound such as ammonium (NH_4^+) or nitrate (NO_3^-) through a series of reactions performed by various microorganisms or high-energy events capable of breaking the triple bond of N_2. These series of reactions form the nitrogen cycle, which is divided into multiple steps, including nitrogen fixation, nitrification, anammox, and denitrification [1]. The individual steps in the nitrogen cycle are explained in the corresponding subsections below.

The nitrogen cycle is a global biogeochemical process that encompasses three primary cycles: atmospheric, marine, and terrestrial cycles. Nitrogen flows from the atmosphere to terrestrial and aquatic ecosystems, while being converted from inert molecular nitrogen to reactive nitrogen forms [10]. The global nitrogen cycle is driven by a range of environmental variables such as solar energy, precipitation, temperature, soil texture, moisture, the presence of other nutrients and atmospheric CO_2 concentrations [11]. These factors collectively regulate the movement and availability of nitrogen within ecosystems on a global scale.

The terrestrial nitrogen cycle represents a crucial component of this global process, focusing specifically on the dynamics of nitrogen within land-based ecosystems. Unlike the broader scope of the global cycle, the terrestrial cycle is concerned only with the movement and availability of nitrogen within terrestrial ecosystems alone. The processes of the terrestrial nitrogen cycle and their relations can be seen in Figure 2.1. Terrestrial ecosystems act as the primary interface for nitrogen interaction with plants within the global nitrogen cycle. The same factors that drive the global nitrogen cycle also regulate the terrestrial nitrogen cycle. For instance, solar energy impacts plant growth, which affects nitrogen demand, while precipitation and temperature influence the movement of nitrogen and microbial activity in the soil. Nitrogen typically moves in three main directions within ecosystems: upward, through processes such as crop uptake and gaseous release; downward, as it leaches into groundwater; and laterally, via both surface and subsurface flows that lead to various water bodies. Soil texture, moisture, and the balance of other nutrients in the soil further impact the retention and accessibility of nitrogen for plants [11].

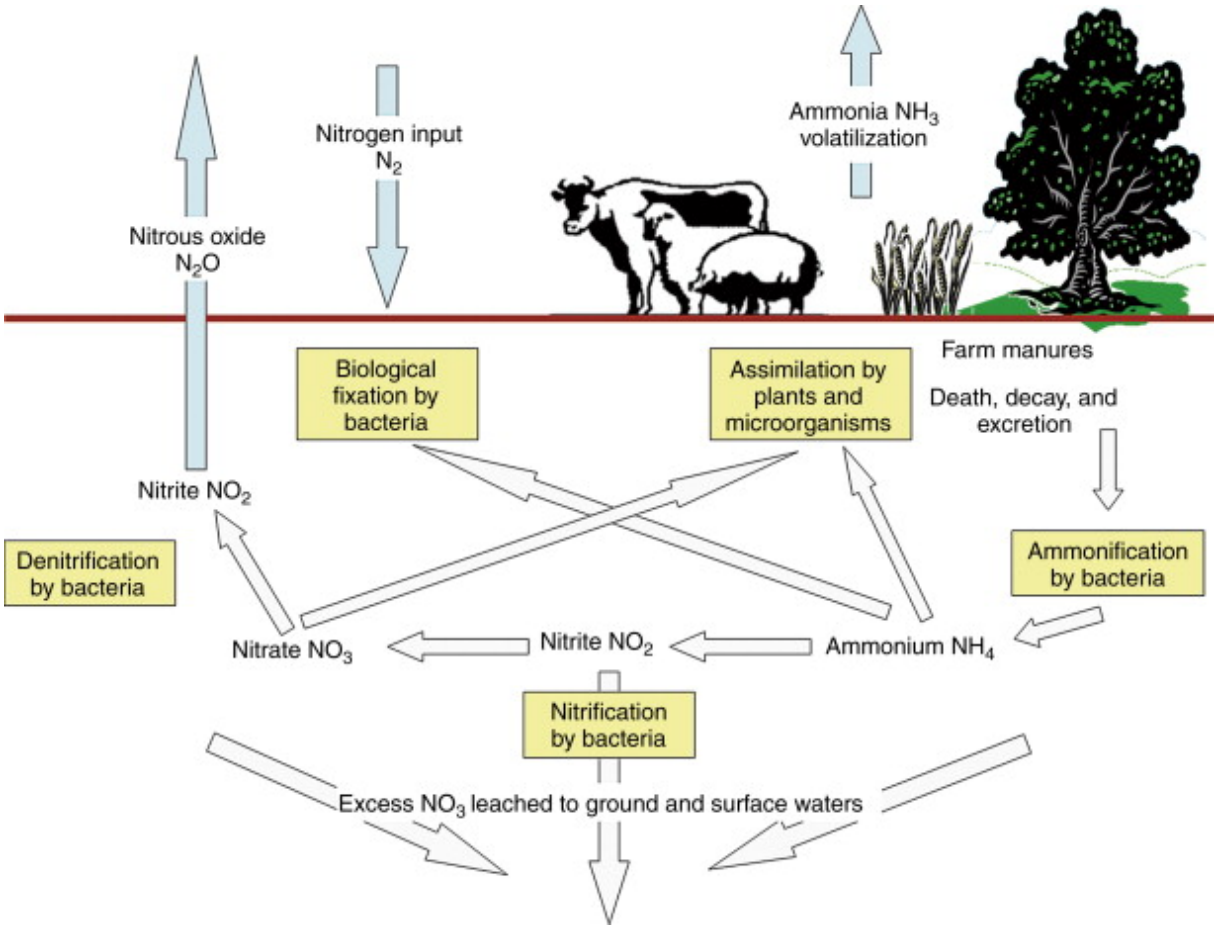

Figure 2.1: Scheme of the terrestrial nitrogen cycle showing the transformation and movement of nitrogen through various biological and chemical processes within a terrestrial ecosystem [11]

2.1.1 Nitrogen fixation

In the nitrogen fixation process, molecular nitrogen (N_2) is converted into biologically reactive ammonia (NH_3) or ammonium (NH_4^+). The main natural source of reactive nitrogen is biological nitrogen fixation, done by nitrogen-fixing microorganisms called diazotrophs. These microorganisms have the unique ability to reduce nitrogen gas into ammonia with an enzymatic complex called nitrogenase. Nitrogenase enzymes are responsible for breaking the triple bond between nitrogen atoms in N_2, using the energy from the hydrolysis of ATP (adenosine triphosphate) as shown in the equation below [12].

$$N_2 + 8e^- + 8H^+ + 16ATP \rightarrow 2NH_3 + H_2 + 16ADP + 16Pi$$

Diazotrophs can live freely in the soil or form symbiotic relationships with certain plants, particularly legumes. In the symbiotic relationship, the microorganisms called rhizobia inhabit the legume root nodules and provide the plant with nitrogen in exchange for carbohydrates [13]. This symbiosis not only benefits plants by providing them with essential nitrogen, but also enriches the soil with fixed nitrogen, which enhances the fertility of the soil and contributes to plant growth and productivity.

In addition to biological fixation, nitrogen can also be fixed through high-energy events such as lightning or forest fires. These events provide the energy necessary to break the strong triple

bond of atmospheric nitrogen, making individual nitrogen atoms available for chemical reactions and transformations [1].

To meet the nitrogen demands of crop production, artificial nitrogen fixation is necessary in addition to natural nitrogen fixation. Anthropogenic processes have become a significant source of fixed nitrogen, more than doubling the amount of nitrogen fixed in the biosphere. Most anthropogenic reactive nitrogen is produced by the Haber-Bosch process, during which nitrogen reacts with hydrogen under high temperature and pressure, resulting in ammonium, as is shown in the equation below. Nitrogen can also be added through the intentional cultivation of legumes and other plants with the ability to fix nitrogen [1]. This additional nitrogen can disrupt the balance of the nitrogen cycle and have negative consequences for the environment, which is explained in the chapter Changes to the nitrogen cycle.

$$N_2 + 3H_2 \rightarrow 2NH_3 + \Delta H(J/mol)$$

2.1.2 Ammonification

Ammonification is a step in the nitrogen cycle, in which nitrogen in organic matter is broken down and converted to ammonium (NH_4^+) or ammonia (NH_3). This process is carried out by decomposers such as bacteria and fungi. The resulting ammonium is then assimilated for the synthesis of amino acids or used in the metabolic processes of these microorganisms. Any excess of ammonium beyond their immediate metabolic demands is excreted into the surrounding environment where it becomes an accessible nutrient for plant uptake or a substrate for subsequent microbial processes, notably nitrification. Ammonification plays an important role in recycling nitrogen from dead organic matter back into the soil. It is a significant factor in plant nutrition as it directly impacts the availability of ammonia for the subsequent nitrification process [14].

2.1.3 Nitrification

Nitrification is a process during which NH_4^+ or NH_3 is converted into nitrites (NO_2^-) and subsequently to nitrates (NO_3^-). This transformation is carried out by specialized groups of microorganisms called nitrifiers, including ammonia oxidizing bacteria, ammonia oxidizing archaea, and nitrite oxidizing bacteria [15]. Ammonia oxidizing bacteria and archaea (also referred to as ammonia oxidizers) are autotrophic microorganisms, meaning that they can produce organic compounds from inorganic sources. These microbes play a crucial role in nitrification by oxidizing ammonia (NH_3) as part of their metabolic processes. In this oxidation, they derive energy from ammonia and generate nitrite (NO_2^-) as a by-product. The resulting nitrite is then used as an energy source by nitrite-oxidizing bacteria, which turn it into nitrate during their metabolic process. The two processes are shown in the following equations.

$$NH_3 + 1.5O_2 \rightarrow NO_2^- + H_2O + H^+$$

$$NO_2^- + 0.5O_2 \rightarrow NO_3^-$$

During these processes, some intermediate by-products can be produced, including nitric oxide (NO) and nitrous oxide (N_2O). Nitrous oxide is typically produced under low-oxygen conditions and its production leads to the loss of nitrogen from the soil. Not only does nitrogen become unavailable for plant uptake as it escapes into the atmosphere, but N_2O is also a potent greenhouse gas [15]. The two steps of nitrification, together with the subsequent conversion of nitrates to N_2 is shown in Figure 2.2.

Nitrogen is often added to the soil in the form of ammonium, which can be readily absorbed by plants. Positively charged ammonium ions adhere to negatively charged clay particles and

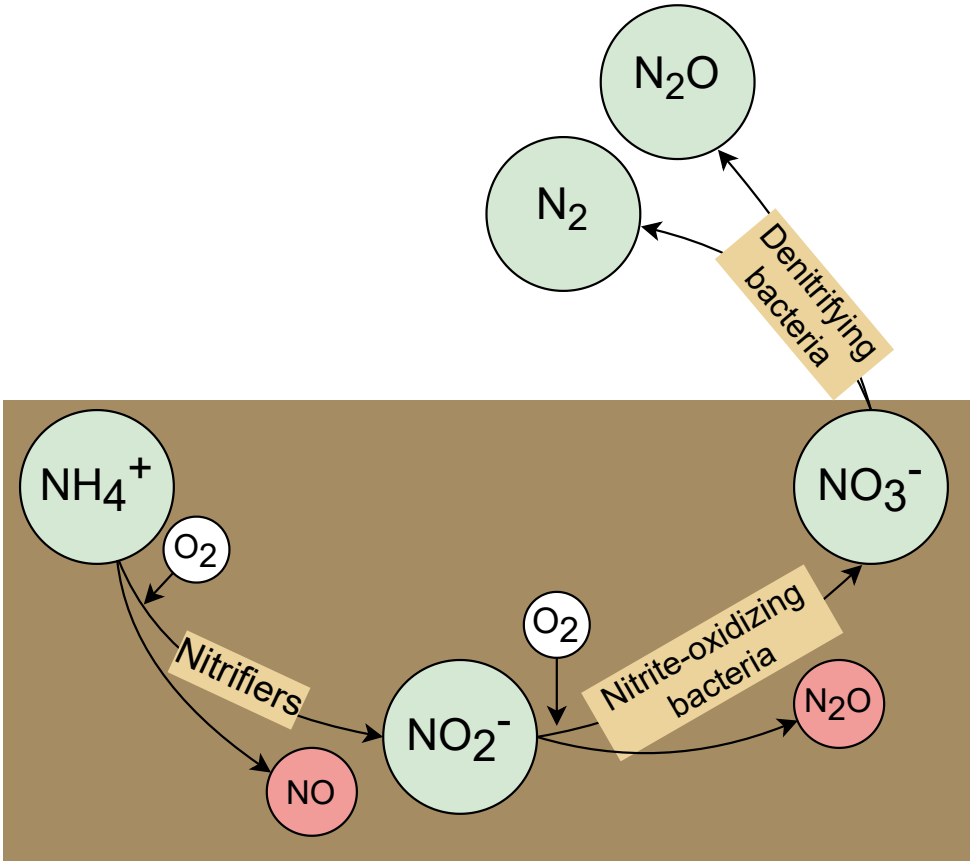

Figure 2.2: Diagram showing the conversion of ammonia to dinitrogen through nitrification and denitrification

organic matter. This interaction immobilizes ammonium, reducing its mobility and reducing its susceptibility to leaching [1]. In contrast, nitrates are fully soluble in water and do not adsorb to clay particles due to their negative charge. This solubility enables them to dissolve readily in water and move downward with infiltrating rain or water from irrigation, increasing the risk of leaching. Because of this, nitrification inhibitors are often added along with fertilizers to slow the transformation of ammonium to nitrate, so that nitrogen is maintained within the soil for better plant uptake.

2.1.4 Nitrogen uptake and assimilation

Due to the large losses of nitrogen through leaching or volatilization, it is often a limiting nutrient for plant growth in both natural and agricultural ecosystems [16]. Being a limiting nutrient means that its availability is a factor that restricts the growth and productivity of plants even if all other nutrients are present in sufficient quantities. The process of nitrogen uptake and utilization involves several steps: uptake via root absorption, assimilation, translocation, and remobilization [17].

Plants have evolved various strategies to thrive under low nitrogen conditions. They have developed sensitive and selective uptake mechanisms and the ability to grow on different nitrogen sources such as ammonium (NH_4^+), amino acids and nitrate (NO_3^-) [16]. They utilize specialized structures such as root hair and root cell membranes to absorb nitrogen from the surrounding soil. The preferred type of nitrogen for plant uptake depends on the specific en-

vironmental conditions and adaptations of the plant species. In acidic soils and rice paddies, ammonium (NH_4^+) is the preferred form for plant uptake, while in climates where nitrification and mineralization are limited, such as arctic regions, plants typically rely on amino acids as their nitrogen source. Plants adapted to alkaline soils and more aerobic conditions most commonly use nitrate [16, 17].

The next step is assimilation, which involves the conversion of absorbed nitrogen, typically in the form of nitrate (NO_3^-), into usable organic compounds for growth and metabolic functions. After nitrate is taken up by roots, it is reduced to nitrite (NO_2^-) in the cytosol by the enzyme nitrate reductase. Next, nitrite is transported to plastids or chloroplasts, where it is further reduced to ammonium by nitrite reductase. This reduction from nitrate to ammonium occurs primarily in root cells, although in cases where NO_3^- uptake exceeds the root assimilation capacity, excess nitrate is transported to the shoot and leaves and transformed there. The resulting NH_4^+ is integrated into amino acids through enzymatic reactions. These amino acids serve as fundamental building blocks for proteins, enzymes, chlorophyll, and other essential molecules that support plant growth, reproduction, and overall physiological functions [16, 18].

Chlorophyll, the green pigment responsible for converting light energy into chemical energy during photosynthesis, plays a significant role in the monitoring of nitrogen uptake through remote sensing and optimizing fertilizer rates. Its unique interactions with light, which are explained in more detail in the chapter Remote sensing, enable us to assess the concentrations of chlorophyll in vegetation and their changes. As plants assimilate nitrogen, leading to the synthesis of chlorophyll, there is increased absorption of light used in photosynthesis. In the case of nitrogen deficiency, chlorophyll synthesis is directly affected, resulting in reduced chlorophyll levels and decreased light absorption [18]. This dynamic relationship between nitrogen assimilation, chlorophyll synthesis, and light absorption forms the basis for the use of remote sensing techniques to detect and respond to changes in plant nitrogen status.

Nitrogen remobilization is a vital mechanism that ensures optimal nitrogen utilization within plants. This process starts with the breakdown of nitrogen-rich compounds, particularly chloroplast proteins, in older leaves or storage organs. The resulting nitrogen-containing compounds, such as amino acids, are then transported through the phloem to growing tissues where they are utilized for the synthesis of new proteins and other essential molecules [17]. This mechanism allows plants to prioritize nitrogen utilization in areas crucial to growth, reproduction, and metabolic functions. Especially during nitrogen deficiency, the chloroplast proteins are broken down to supply nitrogen to essential areas of the plant. This, in turn, leads to a reduction in chlorophyll levels in older leaves of the plant.

2.1.5 Denitrification

Denitrification is a process in which nitrate is converted into gaseous forms of nitrogen, mainly N_2O and N_2. This reduction process is a form of respiration carried out by a diverse group of microorganisms called denitrifiers [19]. Most denitrifiers are facultative aerobes, which means they can switch to anaerobic respiration when oxygen is scarce and use nitrate as an electron acceptor instead of oxygen [20].

$$2NO_3^- + 10e^- + 12H^+ \rightarrow N_2 + 6H_2O$$

In environments with limited oxygen and available nitrate or nitrite, these microorganisms produce denitrification enzymes to facilitate this conversion. However, when reintroduced to oxygen-rich conditions, the activity of the denitrification enzymes is typically inhibited. The regulation of these enzymes varies among different denitrifying microorganisms and their response to oxygen levels [19]. Denitrification occurs in 4 subsequent stages as shown in the

equation below.

$$NO_3^- \rightarrow NO_2^- \rightarrow NO \rightarrow N_2O \rightarrow N_2$$

Ammonia oxidizers can also contribute to the production of N_2 gas under low-oxygen conditions. This process is called nitrifier denitrification [20].

$$NH_4^+ \rightarrow NH_2OH \rightarrow NO_2^- \rightarrow NO \rightarrow N_2O \rightarrow N_2$$

The occurrence of denitrification depends on three criteria: the presence of an energy source for the microorganisms, typically in the form of organic carbon; anoxic conditions within the soil environment; and the availability of nitrate. In addition to these, denitrification is also influenced by factors such as temperature or pH, which play a crucial role in modulating microbial activity [21].

The oxygen levels in the soil, a critical component in denitrification, are influenced by various factors such as irrigation, rainfall, soil type, and other environmental conditions. Excess irrigation or heavy rainfalls can lead to waterlogging, during which the air spaces in the soil fill with water, reducing the availability of oxygen to plant roots and soil organisms [21]. Consequently, denitrification rates tend to increase after irrigation or rainfall events, only to recede once the soil dries out again.

In addition to oxygen, the amount of NO_3^- in the soils directly impacts denitrification rates. Higher levels of NO_3^- usually lead to increased denitrification, as there is more substrate available for denitrifying bacteria to consume in the process. Due to this fact, denitrification rates and N_2O emissions are the highest after fertilization or manure application, as they introduce a significant amount of NO_3^- [21].

The type of soil is another factor that affects denitrification. Less porous peat and clay soils, characterized by their higher water retention capacity, are more susceptible to denitrification, while highly porous sandy soils have a lower denitrification potential [22]. In arable land, human interventions can further contribute to denitrification. Incorporating crop residues, especially those rich in easily available carbon such as sugar beet or vegetables, and the application of manure can increase denitrification activity and N_2O emissions [21].

Denitrification has both positive and negative effects on the environment. On the positive side, it reduces leaching of NO_3^-, contributing to water quality. On the other hand, denitrification is responsible for the loss of nitrogen that could otherwise be taken up by plants and increases the emissions of N_2O, a potent greenhouse gas.

2.1.6 Anammox

Another group of nitrifiers is anammox (anaerobic ammonium oxidation) organisms. Unlike other nitrifying bacteria, anammox bacteria conduct their metabolic processes in the absence of oxygen. Through the anammox process, the bacteria oxidize ammonia to N_2 using nitrite (NO_2^-) as an electron acceptor instead of oxygen. The produced nitrogen gas is not biologically available to plants and is lost from the system through evasion. Therefore, anammox plays a significant role in the removal of nitrogen from various ecosystems, particularly in environments where oxygen levels are low, such as oxygen-depleted zones in oceans, wetlands, and sediments [15, 23]. Furthermore, anammox has found application in wastewater treatment, especially in the treatment of concentrated industrial wastewater [23].

$$NO_2^- + NH_4^+ \rightarrow N_2 + 2H_2O$$

2.2 Anthropogenic changes to the nitrogen cycle

The nitrogen cycle plays a critical role in the survival of all living organisms by facilitating food production. Before the invention of the Haber-Bosch process, food production relied heavily on the recycling of nitrogen from crop residues and manure within the same agricultural area, maintaining a relatively stable level of nitrogen in the ecosystem [11]. Any additional nitrogen sources were also naturally occurring, including guano, a natural fertilizer derived from the accumulated droppings of seabirds, bats or seals on arid islands, and evaporite nitrate deposits in South America, particularly in Chile [24]. However, these sources did not supply enough nitrogen to sustain the rapidly growing human population. Following the breakthrough of the Haber-Bosch process, the ability to synthesize nitrogen-based fertilizers revolutionized agriculture. The transition from reliance on natural sources of nitrogen to industrial nitrogen fixation marked a significant shift in agricultural practices. However, this shift has led to an exponential increase in nitrogen inputs into the environment, disrupting the nitrogen cycle.

Human activities such as fertilizer use, biomass and fossil fuel combustion, deforestation, cultivation of nitrogen-fixing legumes, and industrial processes have significantly altered the nitrogen cycle, pushing it beyond its natural limits. This anthropogenic influence has extended the imbalance in the nitrogen cycle beyond Earth's planetary boundaries. The planetary boundary concept was introduced to define nine key Earth system processes, or „planetary boundaries", that, if crossed, could lead to abrupt and/or irreversible environmental changes, significantly affecting the stability of the Earth system [25]. The planetary boundary value for nitrogen fixation through industrial processes and intentional biological fixation, set at 62 Tg N/year, has been far surpassed. In 2020, the annual fixation rate reached an alarming 226 Tg N/year and continues to gradually increase each year. In comparison, the amount of nitrogen fixed through natural processes is estimated to be 58–128 Tg N/year [3, 26].

Most anthropogenic reactive nitrogen comes from the industrial fixation of N for use as fertilizers, which adds up to approximately 106 Tg N/year in 2020 and an additional 43 Tg N/year produced for industrial processes other than fertilizer use. The industrial nitrogen fixation rate has increased exponentially since the 1940s, when it was nearly zero. The global production of reactive nitrogen between the years 1961 and 2020 can be seen in Figure 2.3. Fossil fuel combustion also affects the nitrogen cycle by releasing nitrogen from long-term geological reservoirs into the atmosphere, currently emitting more than 30 Tg N/year. In addition to fossil fuels, nitrogen is stored in long-term biological storage pools such as forests or wetlands. Activities such as biomass burning, deforestation, and drainage of wetlands could mobilize around 60 Tg/year of stored nitrogen. Additionally, the cultivation of leguminous crops leads to the fixation of around 40 Tg of nitrogen annually [26]. Approximately 75% of the reactive nitrogen generated by human activity is used within agroecosystems. Nevertheless, the majority of this nitrogen does not stay there; instead, it is either removed with the crop or disperses into other systems through processes like evaporation, runoff, or leaching. [24].

It is important to note that different regions contribute differently to the alterations of the nitrogen cycle. Variations in nitrogen production are primarily influenced by diverse economic activities, levels of industrialization, agricultural practices, and regulatory policies. The most significant contributor to reactive nitrogen creation are Asian countries, which produce about 50% of the total anthropogenic Nr [26]. On the other hand, Africa and Oceania have the lowest production rates. Highly industrialized regions, such as parts of North America, Europe, and Asia, often exhibit elevated nitrogen emissions stemming from intensive industrial processes, substantial fossil fuel combustion, and the extensive use of nitrogen-based fertilizers in agriculture. This dependence on industry and agricultural intensity contribute significantly to nitrogen loading in the environment.

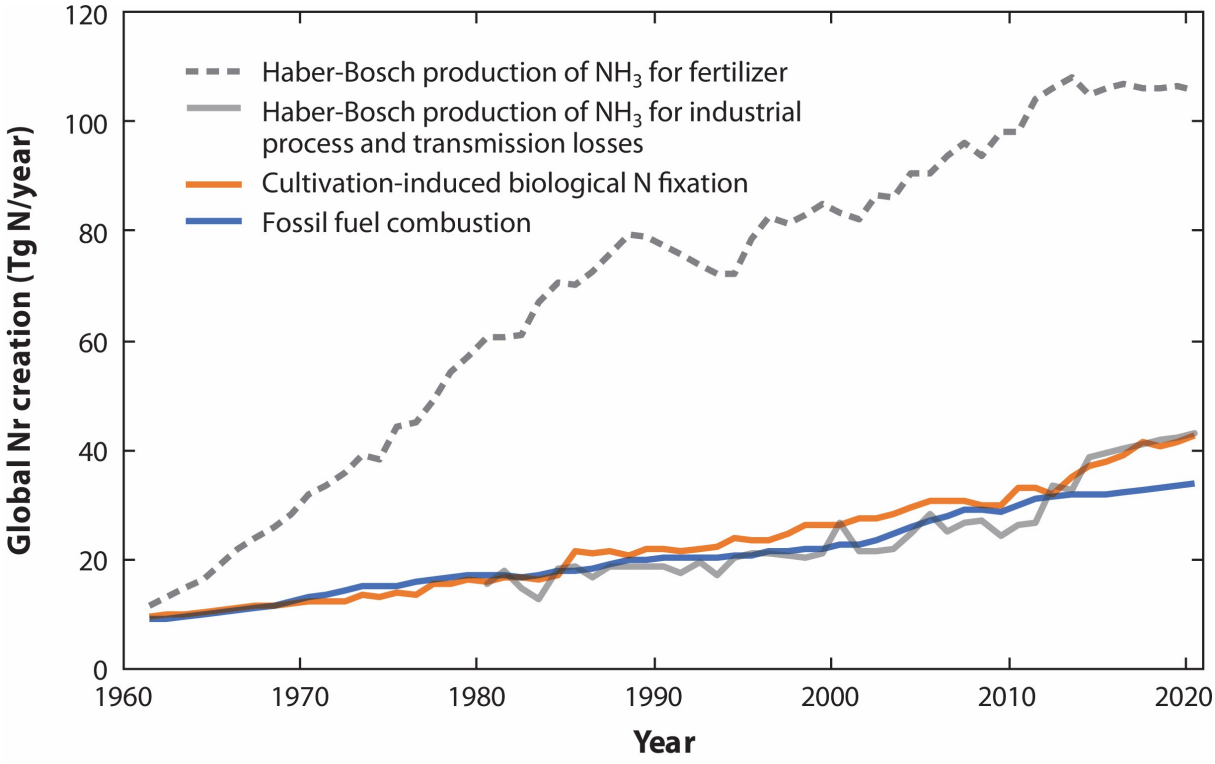

Galloway JN, et al. 2021
Annu. Rev. Environ. Resour. 46:255–88

Figure 2.3: Graph showing global nitrogen (N) creation by different sources: Haber-Bosch Production of NH3 for Fertilizer, Haber-Bosch Production of NH3 for Industrial Processes (HBI), Fossil Fuel Combustion, and Cultivation-Induced Biological N Fixation. The data covers the period from 1961 to 2018, with HBI data available from 1980 to 2018. Estimates for 2019 and 2020 were extrapolated based on the previous ten years' data. [26]

2.2.1 Consequences of the changes

As people produce and input more and more reactive nitrogen into the nitrogen cycle, going beyond what is sustainable, the consequential impact on ecosystems becomes increasingly apparent. Reactive nitrogen, characterized by its high mobility, disperses extensively throughout the environment, cascading through air, water, and terrestrial ecosystems. Despite the ultimate conversion of Nr to unreactive dinitrogen gas, the rapid production of Nr exceeds its conversion rate, leading to its accumulation in many regions [27]. The consequences range from affecting biological diversity, and degradation of air quality to eutrophication and the creation of so-called dead zones [3]. This subsection discusses in more detail the consequences of human-induced changes in the nitrogen cycle, focusing on the atmosphere and aquatic and terrestrial ecosystems.

Aquatic ecosystems

One primary concern revolves around nutrient runoff, where excess fertilizers are washed away by rainfall or irrigation and enter nearby water bodies. In addition, fertilizers can infiltrate the water through a process known as leaching. Nitrate leaching is one of the most important

pathways of nitrogen loss in which nitrates move down through the soil profile and eventually reach groundwater [28]. Leaching occurs when nitrogen inputs exceed crop demand and the nitrogen from applied fertilizer is not used by plants and accumulates in the soil. When large amounts of water, typically from rainfall or irrigation, seeps through the soil, it carries these nitrates along with it.

These pathways carry high levels of nitrogen, primarily in the form of nitrates, along with phosphorus, initiating a phenomenon known as eutrophication. The term eutrophication encompasses excessive nutrient enrichment of water bodies and its effects. It is estimated that up to 40% of the applied nitrogen globally ends up in both surface water and groundwater [11]. Increasing concentrations of nitrogen have been observed in surface waters throughout the world, for example, the concentration of nitrate has more than doubled in the Mississippi River since 1965 and has risen similarly in Norwegian lakes [3]. Nitrate concentrations have also been monitored in wells located in Káraný waterworks situated along the Jizera River in the Czech Republic, which supply Prague with drinking water. Although the measured concentrations vary between different well systems, there is a noticeable trend. On average, the concentration of NO_3^- has increased from 15–20 mg/l in the years 1938-1940 to 104 mg/l in 2011 [29]. As these nutrients accumulate in water, they can promote excessive growth of algae leading to algal blooms. These blooms are not only toxic in some cases, but can also deplete oxygen levels in the water, causing harm to fish and other marine organisms. Furthermore, the decomposition of these excessive plant materials can further deplete oxygen levels [11] and create dead zones, areas in bodies of water with extremely low oxygen levels, where only very few marine organisms can survive. In addition to environmental concerns, nitrates in drinking water pose a threat to human health, being linked to conditions such as methemoglobinemia, also known as 'blue baby syndrome', in infants and stomach cancer in adults [28].

Atmosphere

Anthropogenic alterations of the nitrogen cycle substantially affect the atmosphere, mainly through the release of nitrous oxide (N_2O), nitrogen oxides (NO_x) and ammonia (NH_3). These compounds, which originate from various sources, such as industrial activities, combustion processes, and agricultural practices, significantly impact air quality and pose potential risks to human health [27].

Oxidized nitrogen compounds, specifically nitric oxide (NO) and nitrogen dioxide (NO_2), are created primarily through the combustion of fossil fuels in internal combustion engines and industrial power plants and by burning biomass [30]. Additionally, agricultural fertilization increases the concentration of volatile NH_3 and other nitrogen emissions from the soil. Nitrogen gases in the form of NO or N_2O are produced during microbial denitrification and contribute to atmospheric nitrogen levels. Among these, nitrous oxide holds particular significance as a greenhouse gas and as a contributor to the depletion of stratospheric ozone. With an atmospheric lifespan of approximately 100 years [30], N_2O concentrations are increasing at a rate of 0.2-0.3% per year [3]. Beyond its environmental impacts, nitrous oxide can be harmful to human health, acting as an irritating gas that can cause lung damage when inhaled. Long-term exposure to low levels of nitrous oxide can lead to symptoms such as coughing, headaches, loss of appetite, and stomach problems [27].

As mentioned earlier, nitrous oxide has a very long lifetime and due to this characteristic affects the Earth globally. On the other hand, the highly reactive compounds NO, NO_2 and NH_3 remain in the atmosphere only for a few hours to a few days, undergoing reactions and therefore having a mainly local effect [30]. Nitric oxide participates in the formation of tropospheric ozone, a key pollutant that affects both human health and plant productivity. In addition, the

oxidation of NO results in nitric acid, a crucial component of acid rain. Ammonia enters the atmosphere through volatilization of fertilizer N or as emission from domestic animal waste and biomass burning [3]. Ammonia acts as a primary acid neutralizing agent, helping mitigate the harmful effects of acid rain, but it can also contribute to the formation of fine particles, which have adverse effects on respiratory health [27].

Terrestrial ecosystems

Nitrogen is an essential nutrient for plants, and alterations in its availability can impact plant growth and ecosystem dynamics. Given that reactive nitrogen (Nr) is often the limiting nutrient in most natural and seminatural ecosystems, plants have adapted to soils with low levels of nitrogen. With the addition of nitrogen, these plants are out-competed by more nitrophilic or acid-resistant plants, ultimately resulting in a decline in biodiversity [27]. Experiments across various regions, including North American grasslands, European grasslands, and European heathlands, confirmed that the addition of nitrogen can reduce plant diversity, with certain experiments indicating a more than fivefold decrease in the number of plant species [3].

Although nitrogen is an essential nutrient for plant growth, excessive amounts can lead to nitrogen toxicity. Elevated Nr concentrations can inflict direct foliar damage, especially in lower plants, and long-term high levels of Nr can make them more susceptible to stress, such as frost damage, herbivory, or disease.

To mitigate the negative impacts of excessive fertilizer use, it is crucial to adopt sustainable farming practices such as precision agriculture, where fertilizers are applied in a targeted manner based on the specific nutrient needs of the crops. Implementing nutrient management plans, practicing controlled release fertilization, and promoting organic farming methods can also help minimize the environmental effects of fertilizers.

2.3 Precision agriculture

As discussed in earlier sections, agriculture, particularly the use of fertilizers, can have negative impacts on the environment. Traditional agricultural practices often involve the overuse of pesticides, fertilizers, and water, resulting in water contamination, greenhouse gas emissions, and reduced biodiversity. To address these environmental issues, it is necessary to adopt innovative approaches that balance agricultural productivity with ecological preservation. Precision agriculture (PA), also known as precision farming, is a modern approach to crop cultivation and animal husbandry based on the principles of sustainable agriculture [31].

Precision farming practices consider the heterogeneous characteristics of farmland as opposed to the conventional approach, where the agricultural plot is viewed as a uniform unit. It began to take shape in the late 20th century with the emergence of global positioning system (GPS) technology in the 1970s [32], which provided farmers with the means to accurately map and navigate their fields and laid the foundations for the integration of technology to address the spatial complexity of modern agricultural landscapes. Various techniques have been used to obtain spatial and temporal data on soil, crops, and livestock, some of which are radio, laser, microwave systems, and others. PA uses up-to-date information technologies and data-driven strategies to optimize production processes with the use of sensors, drones, GPS, artificial intelligence, etc.[31]. The collected data are analyzed and used to precisely determine the needs of plants or animals with respect to the heterogeneity of the system. The goal is to maximize yields while minimizing losses, along with optimizing resource use, such as water, fertilizers, and energy.

2.4 Remote sensing

Remote sensing is the process of detecting and monitoring the physical characteristics of an area by measuring its reflected and emitted radiation from a distance, using tools such as unmanned aerial vehicles (UAVs) or satellites [31]. This technology allows for near-real-time assessment of various crop conditions, including the nitrogen status, without the need for sampling and laboratory analysis, while effectively capturing spatio-temporal variability.

Each satellite or remote sensing device is designed with specific purposes and capabilities, leading to variations in the data they capture. Data can vary in terms of spectral, spatial, and temporal resolution and atmospheric correction. Spectral resolution refers to the number and size of spectral bands in which data are collected. In general, the narrower the spectral band and the higher the number of bands, the more precise the results are. However, with smaller spectral bands, a very high sensor sensitivity is required, leading to an increase in the price of the device [31]. Satellites have sensors that can capture data in various spectral bands. Some may have multispectral sensors with a few bands (e.g. Landsat, MODIS), while others might have hyperspectral sensors capturing hundreds of narrow bands (e.g. Hyperion) [33]. Temporal resolution refers to the frequency at which data or information can be obtained from a specific area over time. In the context of satellite imagery, the temporal resolution is influenced by the orbit of the satellite, which determines how frequently the satellite passes over the region of interest [31]. Another characteristic influencing the quality of the resulting data is spatial resolution, the pixel size of the image, which refers to the level of detail in the imagery and the size of the smallest object that can be detected. High spatial resolution means that finer details can be distinguished [31].

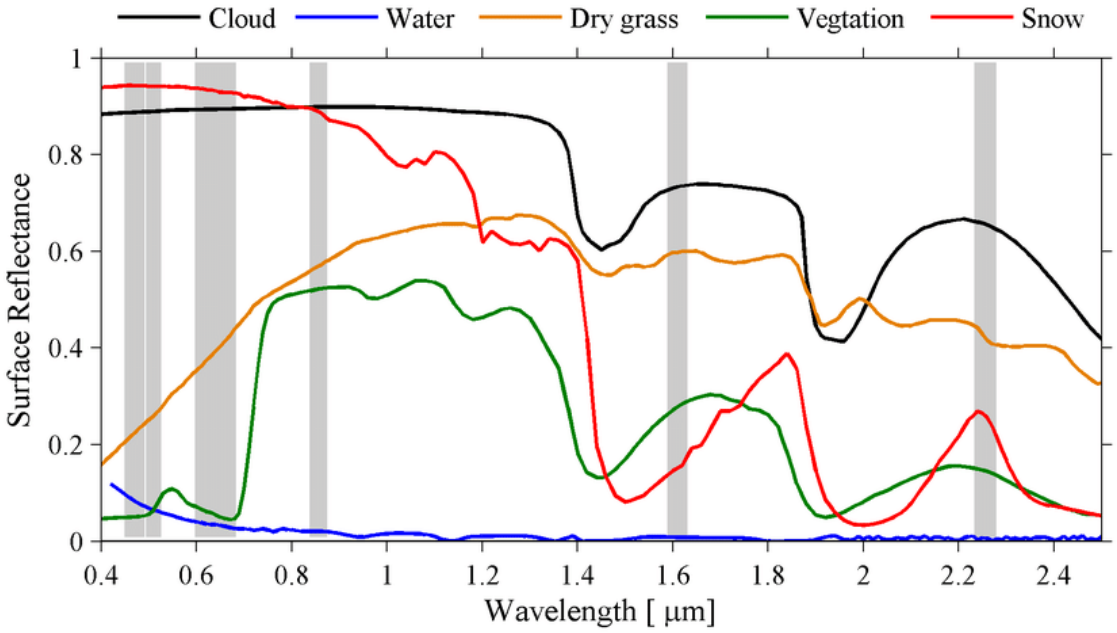

Figure 2.4: Spectral signatures of five distinct surfaces are depicted, with wavelength (µm) represented on the x-axis and reflectance (%) on the y-axis. In the case of healthy vegetation, a noticeable dip in reflectance is observed in the red spectrum, followed by a sudden increase representing the Red Edge. Red Edge is not noticeable on the spectral signature of dry grass. [34]

Due to limited spatial resolution, certain objects cannot be identified solely based on their shape or spatial details. Instead, materials can be distinguished based on their interaction with light. The unique pattern or curve that represents the way an object reflects or absorbs electromagnetic radiation across different wavelengths is called a spectral signature [33]. Healthy vegetation absorbs light in the red (600-700 nm) and blue (400-500 nm) parts of the electromagnetic spectrum for photosynthesis, while reflecting light in the near-infrared (NIR, 780-2500 nm) spectrum. Green light is reflected by chlorophyll, resulting in the characteristic green color of plants [35]. Stress in plants is accompanied by reduced near-infrared reflectance and reduced red light absorption; however, the degree of change in reflectivity is different among different plants. The region with a sharp increase in reflectance between the red and NIR spectrum is known as the Red Edge. This slope is influenced by the amount of chlorophyll in leaves and can be used to determine stress in plants. Non-vegetated surfaces, such as soil and water, have different reflectance patterns [35]. Figure 2.4 depicts the spectral signatures of different surfaces.

Spectral signatures are quantified and characterized using mathematical representations called vegetation indices (VIs). Vegetation index is a numerical value without units that represents the state of vegetation at the particular moment in time when it was obtained. [35] These indices are designed to capture specific aspects of vegetation, such as the amount of chlorophyll and overall plant health. In doing so, they provide valuable insights into the physiological state of plants and can serve as indicators of important plant processes, including nitrogen uptake. It is important to note that the data collected by remote sensing can be distorted by the scattering of solar radiation in the atmosphere, potentially influencing the values of vegetation indices. Therefore, it is crucial to apply atmospheric corrections, which aim to remove or minimize the effects of atmospheric conditions [31].

To effectively convey spatial variations in vegetation health and vigor, vegetation indices are often visualized with color maps, such as the one shown in Figure 2.5. These color maps assign specific colors to different index values, making it easier to interpret the data.

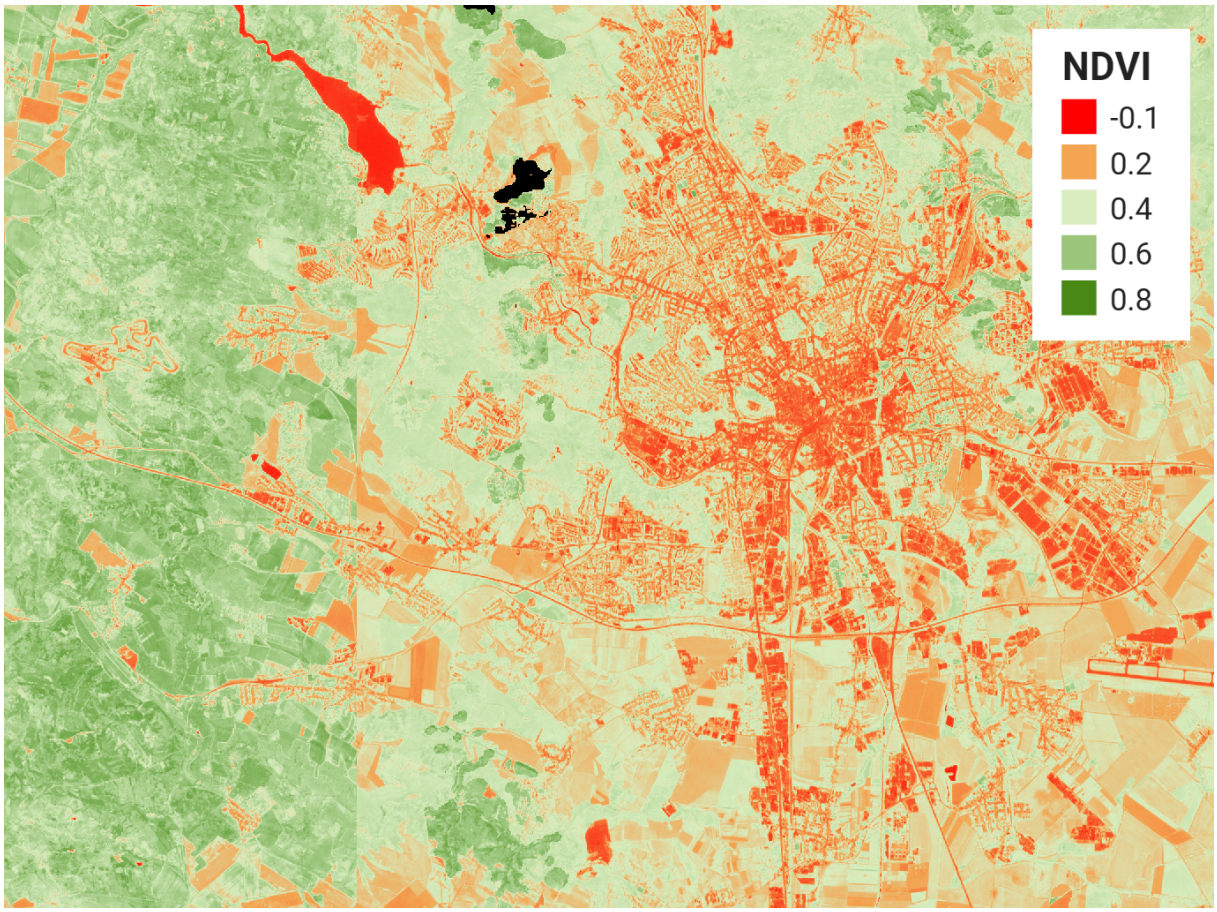

Figure 2.5: Color map showing median NDVI values between march 2023 and July 2023 for Brno. The map was created and exported from Google Earth Engine.

2.4.1 Overview of vegetation indices

The launch of satellites such as Landsat 1 in 1972 enabled the collection of multispectral imagery [33], establishing the foundation for satellite remote sensing and field monitoring using vegetation indices (VIs). These indices serve as crucial tools to assess the health and conditions of vegetation on large spatial scales.

The first vegetation index created to estimate and monitor crop growth is the ratio vegetation index (RVI) proposed by Jordan in 1969 [36]. This index, which is calculated as a simple ratio of red to near-infrared bands, laid the groundwork for subsequent indices. One of the oldest, yet still one of the most commonly used indices is the Normalized Difference Vegetation Index (NDVI), introduced by Rouse et al. in 1974. It bears a strong resemblance to RVI; but instead of being a simple ratio of the red and NIR bands, it is computed as a normalized difference between the two, leading to more precise outcomes. However, NDVI does not correct for atmospheric and soil effects and can easily become oversaturated at higher vegetation densities. This can lead to inaccurate results. Therefore, many other vegetation indices were created to overcome these issues and obtain more precise results. Over the years, researchers have developed numerous vegetation indices that are tailored to address specific challenges and applications. For example, the Soil Adjusted Vegetation Index (SAVI), proposed by Huete in 1988, aimed to mitigate the influence of soil brightness on vegetation detection [36]. Similarly, the Enhanced Vegetation Index (EVI), introduced by Liu and Huete in 1995, offered improved sensitivity to regions of

high biomass density and reduced atmospheric influences compared to NDVI. One of the most recent vegetation indices is the Visible Band-Difference Vegetation Index (VDVI) created by Wang et al. in 2015 [36]. Currently, there are 519 different vegetation indices according to the Index DataBase [37], each tailored to specific purposes and offering varying levels of precision.

Vegetation indices can be categorized based on their calculation formulas, functional requirements, and spectral bands used. NV5 Geospatial Solutions outlines seven categories, including Broadband Greenness, Narrowband Greenness, Light Use Efficiency, Canopy Nitrogen, Dry or Senescent Carbon, Leaf Pigments, and Canopy Water Content VIs [31]. Each category targets specific vegetation properties, such as vigor, nitrogen content, or water status, which are related to wavelengths included in the calculation.

Among the types of VIs, broadband greenness indices, calculated as simple ratios between bands, offer information on the general quantity and vigor of green vegetation [38]. They combine reflectance measurements sensitive to factors such as chlorophyll concentration, leaf area, foliage clumping, and canopy architecture and provide a measure of the overall amount and quality of photosynthetic material in vegetation, which is essential for understanding the state of vegetation for any purpose. Some examples of indices belonging to this group are NDVI, EVI, GNDVI, and SAVI.

Similarly to broadband greenness VIs, narrowband greenness VIs are designed to provide a measure of the overall amount and quality of photosynthetic material in vegetation. Most of these VIs utilize red and near-infrared measurements to capture the red edge of the reflectance curve, providing greater sensitivity to changes in vegetation health [38]. This is especially beneficial in densely vegetated areas where broadband measures can become saturated. The red-edge spectral region is more sensitive to changes in chlorophyll content than the red band. Given the close association between chlorophyll concentration and crop nutrients, numerous indices that assess crop nitrogen status, including nitrogen uptake, are derived from the red edge band [39]. Some examples of indices belonging to this group are MCARI and NDRE.

It is essential to recognize that various external factors, such as site characteristics, crop type, and environmental conditions, can influence the resulting vegetation index values. This means that the effectiveness of a specific vegetation index on one crop type within a particular setting does not automatically ensure similarly favorable outcomes when applied to a different field with a different crop. The context in which a vegetation index is employed must be carefully considered, as variations in external factors can significantly impact the reliability and interpretability of the results.

2.4.2 Vegetation indices used in the practical part

In this thesis, five vegetation indices were used in the analysis:

- Normalized Difference Vegetation Index (NDVI)
- Normalized Difference Red Edge (NDRE)
- Green Normalized Difference Vegetation Index (GNDVI)
- Modified Chlorophyll Absorption in Reflectance Index (MCARI)
- Enhanced Vegetation Index (EVI)

While NDVI, NDRE and GNDVI are simple normalized difference indices, MCARI and EVI are enhanced indices designed to minimize the impacts of soil and atmospheric influences.

NDVI

The Normalized Difference Vegetation Index can be used to assess the amount of green biomass, the leaf area index, the percentage of vegetation cover, plant vigour and health, plant stress, photosynthetic activity, and agricultural crop yield [35]. The formula for NDVI is expressed as the ratio of the difference to the sum of near-infrared (NIR) and red radiation [38], as shown below:

$$\frac{NIR - Red}{NIR + Red}$$

By integrating both NIR and red reflectance, NDVI exhibits a heightened sensitivity to changes in chlorophyll content and overall vegetation health. Elevated chlorophyll activity correlates with increased red light absorption and increased reflectance of NIR light, resulting in higher NDVI values[35]. Typically ranging between -1 and +1, the NDVI values differ between specific surfaces. For example, water surfaces exhibit NDVI values less than 0, bare soils fall between 0 and 0.1, clouds produce values around 0.23, and snow and ice approximately 0.38 [35]. Vegetation generally reaches values between 0.2 and 0.8 [31]. A major disadvantage of this index is the fact that, at certain chlorophyll concentrations, the index becomes saturated, meaning that further increases in chlorophyll content may not produce proportional increases in NDVI [35]. Consequently, this index is most suitable for measuring the conditions of plants in the early and middle stages of growth [40].

NDRE

As proposed by Barnes et al. (2000), the Normalized Difference Red Edge Index is calculated in the same way as the NDVI, but uses the RedEdge band instead of the red band [38].

$$\frac{NIR - RedEdge}{NIR + RedEdge}$$

Red edge is more sensitive to changes in chlorophyll concentrations compared to other bands and is particularly effective in capturing subtle variations in chlorophyll content. As a result, it can be used to identify areas that might benefit from further soil analysis or that may require adjustments to fertilizer application [39]. The Red Edge band tends to saturate later than the red band; therefore, NDRE is more suitable for the middle and late stages of crop growth compared to NDVI [40].

GNDVI

The Green Normalized Difference Vegetation Index (GNDVI) is another modification of the NDVI, but instead of the red band, it is calculated as a normalized difference between the NIR and the green band [38].

$$\frac{NIR - Green}{NIR + Green}$$

According to Gitelson et al. (1996), the green region of the spectrum is more sensitive to fluctuations in chlorophyll levels compared to the red region, making it more suitable for measuring nitrogen in vegetation [31, 35].

MCARI

The Modified Chlorophyll Absorption Ratio Index (MCARI), introduced by Daughtry et al. in 2000, is one of several CARI indices that serves as an indicator of the relative concentration of chlorophyll [38]. MCARI is designed to minimize the combined effects of soil and non-photosynthetic surfaces. It can be obtained using the following equation:

$$((RedEdge - Red) - 0.2 * (RedEdge - Green)) * (\frac{RedEdge}{Red})$$

However, MCARI is still sensitive to background reflectance properties, particularly when dealing with low Leaf Area Index (LAI) or low chlorophyll concentrations. To address this issue, Daughtry et al. (2000) suggested combining MCARI with a soil line vegetation index, such as the Optimized Soil Adjusted Vegetation Index (OSAVI) [41].

EVI

In 1997, Huete et al. introduced the Enhanced Vegetation Index (EVI) as a refinement of NDVI. EVI was specifically designed to address the limitations encountered with NDVI, especially in areas with dense vegetation or where atmospheric conditions significantly influence the measurements. It accounts for residual atmospheric contamination, such as aerosols, and addresses the variability in soil background reflectance [35]. EVI is calculated using the following formula:

$$G * \frac{NIR - Red}{NIR + C_1 Red - C_2 Blue + L}$$

Here, G represents a gain factor, C1 and C2 are coefficients used to correct for aerosol effects in the red band by incorporating information from the blue band, and L is a coefficient that adjusts for the canopy background reflectance (Huete et al., 1997). Initially tailored for the satellite-based MODIS sensor, EVI requires adjustments to its coefficients based on the specific sensor employed. Ideally, EVI values are expected to range from 0 to 1 for vegetation pixels. However, bright features such as clouds and white buildings, as well as dark features such as water, can result in anomalous pixel values in an EVI image. Therefore, it is crucial to first mask out clouds and other bright objects in the image for an accurate analysis [38].

3 Current trends in remote sensing

The evolution of precision agriculture has witnessed major changes since the pioneering work of Schafer et al. (1985) [42], who introduced the concept of „custom prescribed tillage“ - an approach that emphasizes tailoring tillage practices to the specific requirements of crops. This early recognition that customizing for individual crops, soils, and environmental conditions is crucial laid the foundation for subsequent developments in precision agriculture. As GPS technology became more reliable in the 1990s, precision agriculture saw significant advances, and researchers have begun exploring the possibility of using satellite imagery to map soil and crop conditions [43]. Simultaneously, sensors were developed for direct measurement of soil and crop parameters, such as soil organic matter, crop yields, or soil nitrogen [43].

Today, remote sensing plays an increasingly important role in modern agriculture, offering a non-destructive and efficient means of assessing soil and vegetation characteristics, including the estimation of crop nitrogen uptake. The specific applications of remote sensing are explored in the rest of the chapter, specifically focusing on the estimation of crop nitrogen uptake using vegetation indices derived from satellite imagery and spectrometers.

Sharifi et al. [44] used Sentinel-2 satellite data to estimate maize nitrogen uptake in three fields under various climatic conditions in Iran. The research spanned three years (2017-2019) and focused on evaluating various vegetation indices, including SRRE, SR, NDVI, NDRE, TCARI, MCARI, MTVI2 and GNDVI. These vegetation indices were used to create a nitrogen uptake prediction model. The predicted values were then compared with the estimated nitrogen uptake of the destructive biomass samples collected. The study identified the simple ratio red-edge (SRRE) as the top performing index, yielding the highest R^2 (0.91) and the lowest root-mean-squared error (RMSE) values (11.34 kg/ha). The main limitation of this study is that it only considers one crop (maize) and one sensor (satelite Sentinel-2), and therefore the results may not be generalizable to other crops and sensors.

Li et al. [45] conducted field experiments in Germany and China during the period 2007-2011 to optimize vegetation indices to estimate canopy nitrogen uptake in corn and wheat. Corn and wheat canopy reflectance was measured using a handheld field spectrometer and evaluated using two widely used indices, NDVI and RVI, along with seven three-band indices - all using the red-edge band known for its sensitivity to chlorophyll content and N uptake. Data sets for wheat and corn were randomly divided into two sub-data sets: 75% to establish regression models between spectral indices and N uptake and 25% for model validation. The central bands suitable for assessing canopy N uptake for corn, wheat and for corn and wheat combined were determined. The optimized three-band N planar domain index (NPDI) provided the most accurate predictions, achieving an R^2 of 0.86 and the lowest RMSE (20.1 kg N ha–1) and relative error (RE, 18.7 %). The main contribution of this study is that it proposes a new vegetation index (NPDI) that can effectively estimate canopy nitrogen uptake for both corn and wheat and optimizes central bands for different crops and regions. The main limitation of this study is that it relies on field measurements of canopy reflectance taken with a handheld spectrometer, which may not represent the spatial and temporal variability of crop nitrogen uptake at larger scales.

Fiorio et al. [46] focused on estimating the nitrogen content of leaves in sugarcane using hyperspectral reflectance data. The experiment was carried out in Brazil during the 2014-2015 harvest. Hyperspectral data was obtained using a laboratory spectroradiometer, and the leaf nitrogen content (LNC) was analyzed. The obtained values were used to create spectral models through Partial Least Squares Regression (PLSR) analysis. Acceptable models, with $R^2 > 0.70$ and RMSE < 1.41gkg-1, were generated, with the most robust models derived from visible spectra (400-680 nm) and red edge (680-750 nm) bands. These models were employed for

nitrogen prediction in different periods from calibration and validated using leave-one-date-out cross-validation (LOOCV). In particular, the visible (400-480 nm) and red edge (680-750 nm) bands were of utmost importance in predicting nitrogen uptake through spectral data. This study focuses on the leaf nitrogen content, which is related to nitrogen uptake. It can be used to optimize nitrogen application rates similarly to nitrogen uptake by using models that relate leaf nitrogen content to crop growth and yield. However, the leaf nitrogen content may not capture the effects of nitrogen on other plant organs or processes. Additionally, the study uses laboratory measurements of leaf reflectance, which may not match field or aerial measurements due to variations in illumination, viewing angle, and background noise.

Although the studies differ in crops, locations, and sensors (satellites or spectrometers), they share some common methods and findings. Two of the studies used vegetation indices, such as NDVI and red-edge indices, to assess crop nitrogen uptake, demonstrating their applicability. Additionally, the use of remote sensing technology, whether through satellites or spectrometers, allowed for non-destructive data acquisition. Various modeling techniques were used to predict nitrogen uptake or nitrogen content values based on vegetation indices, all of which showed promising results. Evaluation of different climatic conditions (Sharifi et al. [44]) and nitrogen application rates (Li et al. [45]) highlights the importance of considering environmental factors in nitrogen uptake estimation. However, the studies did not consider the effects of other factors, such as soil moisture, temperature, and phenology, which can also affect nitrogen uptake.

4 Goal of the thesis

In common agricultural practices, the excessive application of nitrogen fertilizers leads to environmental pollution, such as water contamination and greenhouse gas emissions, and economic losses. Remote sensing technology offers a promising approach to optimize nitrogen fertilizer application rates by providing a quick and efficient means of assessing nitrogen uptake. Multiple studies have demonstrated the possibility of using remotely sensed vegetation indices for nitrogen status assessment, crop yield predictions, and others.

This thesis investigates the use of remote sensing technology, specifically using Sentinel-2 satellite imagery, to adjust the application of nitrogen fertilizer in agriculture by monitoring and predicting nitrogen uptake. The study was carried out in Oensingen, Switzerland, and the analyzed crops were grass-clover mixture and winter wheat. The central aim of this work is to compile a comprehensive data set that includes both manually measured nitrogen uptake data and the corresponding vegetation index values. The specific objectives are as follows:

- To measure Leaf Area Index (LAI), crop height, nitrogen concentration and biomass weight of the crops and to calculate the nitrogen uptake of the crops
- To obtain satellite images using Google Earth Engine and calculate the selected vegetation indices (NDVI, NDRE, GNDVI, MCARI, EVI)
- To assess the relationship between satellite-derived vegetation indices and crop characteristics, including nitrogen uptake, through correlation and regression analysis
- To create and validate a prediction model capable of estimating nitrogen uptake based on vegetation index data

The ultimate goal of this research is to develop an efficient tool to predict nitrogen uptake in crops using remote sensing technology. The prediction model could guide precision nitrogen management, reducing the negative impacts of over fertilization.

5 Used methodology

This chapter outlines the methodology used in this study. It begins with a description of the site where the measurements were taken, followed by an explanation of the sampling procedures. The methods used to measure the Leaf Area Index (LAI) and crop height are then detailed. Next, the chapter covers the sample analysis process and the calculation of vegetation indices. The programming language R is introduced, along with any additional libraries used for the analysis. Finally, the correlation and regression analysis and the creation of the prediction model are described.

5.1 Study site description

The sampling and remote sensing analysis was carried out at the Oensingen field site in Switzerland (longitude (WGS 84): 7°44'01.5 E, latitude (WGS 84): 47°17'11.1 N), which serves as an experimental farmland with extensive management. It is a part of the Swiss FluxNet, a network of flux sites in Switzerland that measures greenhouse gas fluxes at the ecosystem scale using the eddy-covariance method. The ecosystem sites belonging to Swiss FluxNet, including the Oensingen site, are shown in Figure 5.1. Aligned with the Swiss integrated management framework of the Proof of Ecological Performance, the Oensingen site follows a typical crop rotation cycle, predominantly featuring winter wheat cultivation every other year with other crops grown in the intervening years.

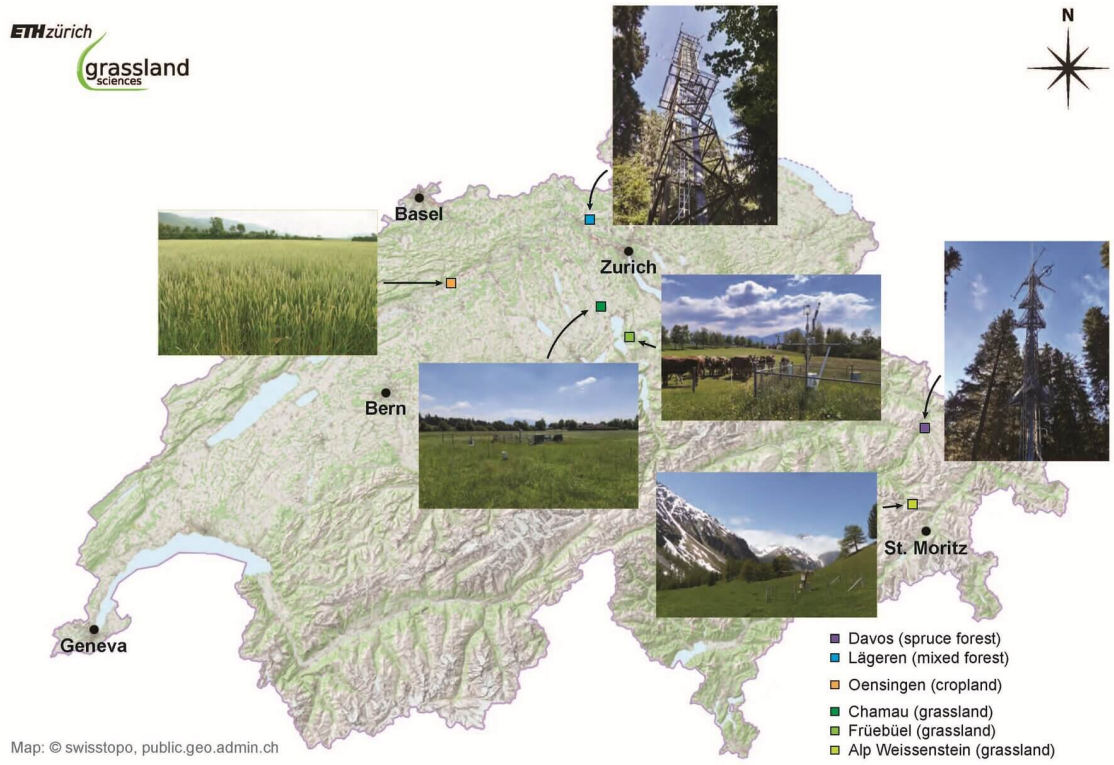

Figure 5.1: Map illustrating the distribution of ecosystem flux measurement sites across Switzerland [47]

The collection of samples was conducted during my internship at ETH Zürich between June and August 2023, which coincided with the cultivation of winter wheat. Additionally, biomass weight and nitrogen concentration data were provided for the years 2021 and 2022, representing the time period when the site operated as a grassland. The grass-clover mixture, consisting of red clover (*Trifolium pratense*), white clover (*Trifolium repens*), orchard grass (*Dactylis glomerata*), meadow fescue (*Lolium pratense*), English ryegrass (*Lolium perenne*), and timothy grass (*Phleum pratense*), was sown in August 2020. The grass was cut regularly at intervals of 1-2 months, 4 times a year. Shortly after the removal of the grass, winter wheat was sown in November 2022. Mineral fertilizer and slurry were applied in February and April 2023, with harvest conducted in July of the same year.

During the period from 2021 to 2023, the mean annual precipitation was 1216.1 mm, with an average yearly temperature of 10.6 °C, as recorded by the MeteoSwiss station in Wynau. The soil of the study site falls under the Cambisol / Gleysol classification, characterized by a silt loam texture, with a pH of 5.3 in the topsoil [48].

5.2 Data collection

This section focuses on the process of collecting data essential for the analysis. Information on the sampling process used for winter wheat collection and its subsequent analysis of nitrogen concentration is provided, together with methods used to measure Leaf Area Index (LAI) and crop height. The acquisition of satellite images and the pre-processing necessary to calculate vegetation indices are also described.

5.2.1 Winter wheat sampling and sample processing

To obtain information on nitrogen uptake of crops, the above-ground biomass of winter wheat was sampled. In the beginning, it is important to carefully choose the sampling scheme and method and then follow the procedures accordingly. This part is crucial because correctly performed sampling allows one to obtain information on nitrogen intake throughout the entire plant population, which is key for determining fertilization needs and optimizing plant nutrition.

Before sampling was performed, the site was divided into four quadrants, with the flux station positioned in the center, which is illustrated in Figure 5.2. Dividing the site into quadrants ensures a more balanced representation of the overall conditions, as each quadrant represents a distinct section of the field. This allows for the inclusion of variations in soil characteristics, microclimates, and other spatial factors that can influence winter wheat growth and nitrogen uptake. Furthermore, this approach ensured that the sampling locations were distributed across the field. To maintain impartiality and equal representation, a random sampling method was used. This approach involves selecting samples without any specific pattern or bias, ensuring that every unit of the population has the same chance to be included in the sample.

Biomass sampling was always conducted shortly after rainfall, a time when denitrification activity peaks and nitrogen availability to plants is enhanced. To ensure consistency in the sample size, a sampling frame with a defined area of 0.1 m^2 was used. For each sample, the sampling frame was randomly tossed behind my back to ensure an unbiased selection. The winter wheat contained within the frame upon landing was collected with scissors and then stored in a bag with the corresponding quadrant and sample number. Each bag was marked with the date, sampler's name, study site ID, quadrant, and sample number to maintain proper organization and prevent any potential mixing of samples. From each quadrant, three random samples were collected, resulting in a total of 12 samples per sampling date.

Figure 5.2: Division of the Oensingen site into 4 quadrants for sampling purposes. The yellow line indicates the borders of the field, while the red line borders the area of sampling together with each quadrant. The satellite image was obtained from Swisstopo.

Subsequently, each sample was subjected to a two-step process: initially, it was weighed in its fresh state and then weighed again after drying for five days at 60°C. Data for each sampling date were precisely documented in dedicated Excel sheets. Once dried, the samples were prepared for analysis of nitrogen concentrations. First, the biomass was crushed into smaller pieces, after which a subsample was finely ground to powder using a ball mill (MM200, Retsch, Germany). The powdered material was then carefully weighed in small tin capsules in preparation for the subsequent analysis of nitrogen concentrations.

5.2.2 Analysis of nitrogen content

The preprocessed above-ground biomass samples were subjected to elemental analysis using the Flash EA 1112 series elemental analyzer (Thermo Italy, formerly CE Instruments, Rhodano, Italy). This instrument is specifically designed for elemental analysis, including determination of the nitrogen concentration by dynamic flash combustion of the sample [49].

Elemental analysis is an analytical technique that is used to determine the elemental composition of chemical compounds. It involves the identification and quantification of individual elements present in a sample. In this case, the analyzer was employed to determine the nitrogen concentration in the above-ground biomass samples, but it is also commonly used to determine the concentrations of carbon, hydrogen, and sulfur. During analysis, the sample undergoes combustion in a reactor, producing oxides of the present elements. These gases are then separated by chromatographic columns and detected using a thermal conductivity detector [49, 50]. After

the analysis is completed, the analyzer provides nitrogen concentrations, displayed as weight percentages.

As a result, 12 nitrogen concentration values were obtained per sampling date. In addition to the results of the current analysis, data from previous years were also provided. However, these only included four values per date (one per each quadrant). The dry biomass weight and nitrogen concentration were later used for the nitrogen uptake calculation.

5.2.3 Leaf Area Index and crop height measurements

The amount of foliage in a plant canopy reflects various factors such as water and nutrient use, microclimatic conditions, and management practices such as fertilization. The plant canopy foliage content is quantified using the Leaf Area Index (LAI), a dimensionless measure that represents the ratio of the total area of one side of leaf tissue to the ground surface area [51]. This index serves as an indicator of plant health, vigor, and canopy density. Higher LAI indicates a greater amount of leaf cover relative to the soil area and may indicate higher photosynthetic activity and plant productivity. LAI can be measured by different methods, including direct measurements, such as harvesting and measuring leaves, or indirect methods that rely on various indicators that allow LAI to be estimated [51]. The most frequently used indirect methods are optical methods that are based on the Lambert-Beer law.

In this case, the Leaf Area Index was measured indirectly using the LAI-2000 Plant Canopy Analyzer (LI-COR Biosciences, USA). The LAI-2000 operates on the principle of measuring the amount of light that infiltrates the canopy. It does so using a fisheye optical sensor positioned just above the ground level, which captures the incoming light from various angles. As the density of leaves in the canopy increases, less light reaches the sensor, and the Leaf Area Index (LAI) also increases [52]. When taking measurements using the LAI-2000, the LAI of the sky without any cover was first measured to ensure that the resulting value would be zero, as there is no leaf cover. Subsequently, the index was measured six times within each quadrant, resulting in a total of 24 data points that were then averaged to obtain the representative value. It was crucial to shade the area of measurement as direct light can influence the final value.

Measurement of the leaf area index together with analysis of nitrogen uptake provides a comprehensive assessment of plant growth, photosynthetic efficiency, and nutrient management. By correlating LAI with vegetation indices, the effectiveness of nitrogen utilization by plants can be evaluated, which can help optimize nutrient management practices.

In addition to LAI, crop height was measured to obtain a more complete understanding of plant growth dynamics and nutrient utilization. By measuring height at different stages of the plant's life cycle, the growth rate can be monitored, and the measured values can be compared with the expected ones. Stress factors such as lack of nutrients, water, diseases, or pest infestations can thus be revealed. Crop height also serves as a tangible indicator of the accumulation of above-ground biomass and the distribution of nitrogen within the canopy.

The crop height measurements used in this thesis were obtained using a cardboard board and a tape measure. The board was carefully placed on the vegetation canopy, and then the height from the ground to the board was measured and recorded. This process was repeated six times per quadrant, resulting in a total of 24 values per date.

5.2.4 Remote sensing data acquisition

Alongside manual sample collection and analysis, satellite imagery was used to assess nitrogen uptake of the vegetation cover. This was achieved by calculating vegetation indices using Google Earth Engine (GEE), a cloud-based platform developed by Google equipped with vast amounts

of satellite imagery and geospatial datasets. Designed for analysis, processing, and visualization of geospatial data, GEE can be used for a wide range of applications in earth observation, environmental monitoring, land use planning, disaster management, agriculture, forestry, etc. Data can be accessed through a web-based interface and the JavaScript Application Programming Interface (API), which enables users to work with the data in Google Earth Engine using programming code written in JavaScript [53]. Google Earth Engine can be used to obtain vegetation indices by applying calculation algorithms on multispectral satellite imagery, such as Landsat and Sentinel data.

In the analysis of vegetation indices, the harmonized Sentinel-2 Level 2-A images were accessed from the Google Earth Engine database. Sentinel-2 was chosen mainly for its temporal and spatial resolution, which offers finer detail compared to other publicly available satellite data. The Sentinel-2 images are captured every five days, and most bands have a spatial resolution of 10 meters, except for the RedEdge band, which provides a resolution of 20 meters. For comparison, Landsat images are taken at a 30-meter resolution. This difference can significantly impact results, especially when analyzing smaller areas, such as in this case.

To prepare the Sentinel-2 images for analysis, they were filtered based on their acquisition dates, only keeping images captured between 1st January 2021 and 28th November 2023 which were relevant to the analysis of winter wheat and grass cover. The images were cropped to the boundaries of the study site by importing a georeferenced shapefile created in Geographic Information System (GIS) software. The shapefile acts like a digital map, specifying the geographic extent of the study site. One significant challenge in processing satellite images was the presence of bright white objects, such as clouds or snow cover, which can distort the values of vegetation indices. To mitigate their influence, a cloud masking technique was employed using the s2cloudless image collection available in GEE. This process involves identifying and removing cloud-covered pixels from being included in the computation. The cloud masking is demonstrated in Figure 5.3, which contains an image before and after the cloud masking was applied. In addition, images with snow cover exceeding 20 % of the image area were also excluded. Given that the Sentinel-2 program operates with a constellation of two satellites, Sentinel-2A and Sentinel-2B, the database often contains two images captured on the same date. Having one image per day is sufficient; therefore, only the image with the lower cloud cover from the pair was kept, since it would have a clearer view of the Earth's surface. During the selected time period, the satellite took in total 401 images. This number has been reduced to 68 throughout the filtering process.

After filtering was performed, the selected vegetation indices NDVI, NDRE, MCARI, EVI, and GNDVI, which are described in more detail in Subsection 2.4.2 Vegetation indices used in the practical part, were computed using their respective equations. The final values were produced by taking the mean index value of the whole field for the day of image acquisition. Finally, the results were exported as a CSV file for further analysis.

5.3 Data analysis

This chapter is dedicated to the preprocessing and analysis of the collected data and explains the software and methods used. This includes the creation of time-series plots and an investigation of the relationship between nitrogen uptake and vegetation indices through correlation and regression analysis and the development of a prediction model. It describes the fundamental concepts of correlation and regression, followed by a detailed explanation of the functions used in R for analysis.

Figure 5.3: Cloud masking application on an image from 14th April 2022. Left side - image before cloud masking was applied, right side - image after cloud masking was applied. The Oensingen study site is depicted in green color.

5.3.1 Programming language R and R studio

R is a programming language used for data analysis and visualization. It provides an extensive range of statistical techniques, including linear and nonlinear modeling, classical statistical tests, and time-series analysis [54]. One of its most valuable characteristics is its extensibility. Through the installation of libraries, users can enhance its functionality by integrating various additional features to suit specific analytical needs. Most of these packages, which were created by other users, are available through CRAN (the Comprehensive R Archive Network) and other sources such as GitHub.

RStudio is an integrated development environment (IDE) for the R programming language, providing a user-friendly interface to write, run, and debug R code.

Libraries used during the analysis

During the analysis, a variety of additional libraries were imported into RStudio. These included extensions of existing functions as well as entirely new functions and visualization tools.

The first library that was imported is data.table, a package that improves the fundamental data.frame structure in R. It enhances data manipulation capabilities by providing concise syntax for tasks such as file reading and writing, subsetting, grouping, and aggregating large datasets. It offers improved speed and efficiency, particularly when handling large data sets [55].

Another package for data manipulation used during analysis is called dplyr, which enables filtering, selecting specific columns, arranging data, and joining data sets [56]. One of the most important features that dplyr adds is the piping operator, which enables users to chain multiple functions together, reducing the need for intermediate variables and improving code readability.

The next library is fuzzyjoin, an invaluable tool for performing fuzzy matching and joining operations in R. Fuzzy matching allows matching records in datasets that are not identical but similar, based on specified criteria such as string similarity or distance metrics [57]. This was especially useful when merging data sets containing values of nitrogen uptake and vegetation indices.

To create visually appealing and custom graphs, the packages ggplot2 and ggthemes were used. The ggplot2 library allows users to create a wide range of graphs, including scatter plots, bar charts, histograms, and more. All aspects of graphs can be easily customized, from colors

and shapes to labels and themes, to effectively communicate data insights [58]. In combination with ggplot2, ggthemes provides additional themes and color palettes to further enhance the appearance of the plots. Another extension of ggplot2 used is GGally, which adds even more types of plots and customization options.

It is possible to create a linear regression model in R without the use of an additional library. However, for the performance validation of the model, the caret library was used as it can significantly simplify the process and is more reliable. The caret package, short for Classification And REgression Training, is an R package designed to optimize the process of model training, tuning, and performance evaluation [59]. It provides functions for performing various cross-validation techniques, including the Leave-One-Out Cross-Validation (LOOCV) which was used in this work.

Other libraries used were stringr [60] for string manipulation and tidyr [61] for data cleaning.

5.3.2 Creation of time-series plots

Time series of nitrogen uptake and vegetation indices are valuable for monitoring, analysis, and understanding changes in vegetation health over time. The plots help to visualize trends, patterns, and fluctuations in both nitrogen uptake and vegetation indices over time. Sudden increases or decreases in their values can indicate environmental stress, such as drought, pest infestation, or nitrogen deficiency. In addition, trends in values over longer periods of time can highlight gradual changes in vegetation health that can indicate soil degradation or environmental pollution.

The time-series plots were created in R Studio using the ggplot2 library. To accomplish this, nitrogen uptake data and all vegetation indices were imported into R and organized into data frames. These data frames included a column with the date of data collection and a column containing the corresponding values.

In the previous chapter, the crop sampling and analysis process was discussed, from which the biomass weight and nitrogen concentrations for each quadrant were obtained. These parameters were used to calculate nitrogen uptake. Following the import of these data into R Studio, any NA values were removed and a nitrogen uptake column was added to the data frame. Nitrogen uptake in g/m^2 was calculated using the formula:

$$(dry - tara \times 10) \times (\%Ncorr./100)$$

where dry-tara is the dry weight of biomass in $g/0.1m^2$ and %N corr. represents the nitrogen concentration in weight percentage. After this was done, the mean nitrogen uptake for the entire field was calculated per date. Since the dataset included nitrogen uptake data for both grass and winter wheat, a column indicating the type of crop was added. Table 5.1 presents the data on the mean nitrogen uptake per field for grass and winter wheat collected on various dates. The columns of the table detail the date of measurement, the dry weight of the samples in grams, the corrected percentage of nitrogen (% N corr.), the nitrogen uptake and the crop.

Similarly, the values corresponding to each vegetation index were imported and organized into five separate data frames. Values very close to zero were removed because they may be the result of cloud or snow interference and probably do not represent the state of vegetation well. Specific thresholds were established to filter these insignificant values: a minimum of 0.1 was set for NDVI, NDRE, GNDVI, and EVI, while for MCARI, which generally exhibits lower values, a threshold of 0.01 was used. The plots have the same structure as those that illustrate N uptake, except for the time extent, which is 30th March 2021 to 16th October 2023. Individual plots were created for each index, displaying values per field and per quadrant. In addition, a combined graph was generated that presents all indices simultaneously to highlight their differences.

Table 5.1: Mean Nitrogen Uptake

Date	Dry Weight (g)	%N Corr.	Mean N Uptake	Material
2020-10-19	5.1500	3.6724	1.8802	grass
2021-05-26	66.5350	1.6819	11.0675	grass
2021-07-20	54.0575	1.9491	10.5621	grass
2021-09-02	33.6175	2.5087	8.4949	grass
2021-10-19	25.6225	3.3031	8.6463	grass
2022-05-10	44.7550	2.4457	10.8053	grass
2022-06-27	33.5050	2.6858	9.1360	grass
2022-08-08	23.4500	2.8714	6.7255	grass
2022-09-19	11.1225	3.6013	4.0209	grass
2022-12-13	4.3517	3.2523	1.3523	winter wheat
2023-02-07	3.9867	3.3363	1.3089	winter wheat
2023-03-17	6.5617	4.0697	2.6571	winter wheat
2023-04-14	19.1483	3.2388	6.0642	winter wheat
2023-05-19	79.3208	1.6666	13.2026	winter wheat

5.3.3 Correlation and regression analysis using R Studio

A linear model was used to analyze the relationship between nitrogen uptake and vegetation indices. Linear models assume a linear relationship between the variables, which is a type of relationship characterized by changes in one variable being linearly reflected in changes in the other [62]. In addition to the main analysis, the relationship between vegetation indices and other measured variables, including dry biomass weight, nitrogen concentration, LAI, and crop height, was evaluated. In statistical modeling, variables can be classified as independent or dependent variables. A dependent variable is the one that is being predicted or explained and its values depend on the changes in the independent variable [63]. In this case, vegetation indices were the independent variable and nitrogen uptake, dry biomass, nitrogen concentration, LAI, and crop height were the dependent variables. Within this model, correlation and regression analyses were employed to further explore the connection between these variables.

Correlation analysis is a statistical technique that helps assess the presence, nature, strength, and direction of associations between two quantities. In R, the cor() function facilitates the evaluation of this relationship by computing the Pearson correlation coefficient (r), which ranges between -1 and +1. A value of ± 1 signifies a perfect degree of association between the two variables, with a positive sign indicating a positive relationship and a negative sign indicating a negative one. As the value of the correlation coefficient approaches 0, the association weakens [64]. It is important to note that while correlation analysis can reveal potential associations between variables, it does not imply causation. To provide additional clarity, a table of graphs was generated with the help of the GGally package, showing the relationship between all variables through scatterplots and their correlation coefficients.

Similarly to correlation, regression analysis is a statistical method used to examine the relationship between a dependent variable and one or more independent variables. In linear regression, a straight line of best fit is established to depict the relationship between variables, with the slope of the line indicating how changes in the independent variable impact a change in the dependent variable [65]. The ordinary least squares (OLS) approach was used to find this line that best fits the data by minimizing the sum of the squared differences between observed and predicted values. The coefficient of determination R^2 was used to quantify the degree to which the model predicts an outcome. Ranging from 0 to 1, it measures the proportion of

variance in the dependent variable (for example, nitrogen uptake) that is predictable from the independent variables (vegetation indices). The closer the R^2 value is to 1, the better the model is at making predictions [66].

A more comprehensive understanding of the relationship between variables can be provided using both correlation and regression analysis. Correlation measures the strength and direction of the linear relationship. However, correlation does not imply causation nor can it be used in case of a non-linear relationship between the variables. Regression analysis goes a bit further by quantifying the relationship between dependent and independent variables and providing an equation that can be used to make predictions.

To construct the linear model, the data sets containing vegetation indices were merged with dry biomass weight, nitrogen concentration, LAI, crop height, and nitrogen uptake. Since satellite image acquisition did not always align perfectly with crop sampling dates, the variable values were combined within a 7-day window using fuzzy matching. After assigning the value of the vegetation index to each value of nitrogen uptake and other variables, the data could be inserted into a linear model. The lm() function in R was used to fit the linear regression model to the dataset, determining the coefficients (slope and intercept) of the regression line, while also calculating the coefficient of determination and other characteristics. Following this, a scatter plot was generated that visualizes the relationship and includes the model equation, the coefficient of determination, and the Pearson correlation coefficient.

5.3.4 Development and validation of prediction model in R Studio

The linear regression model described previously was used to predict nitrogen uptake values based on vegetation indices. Linear regression was chosen mainly because it is relatively simple, produces easily interpretable results, and can often provide reliable predictions with relatively small amounts of data.

The evaluation of a model is crucial to assess its performance and reliability. The performance of a model is evaluated by measuring how well the predictions made by the model match the observed data. Typically, this involves dividing the data set into training and testing sets. The model is built using only the data in the training set and then used to make predictions on the testing set to see how well it performs on unknown data. However, the results of this method can vary depending on how the data set was separated. Additionally, when working with very small data sets, such as in this case, splitting the data may not be feasible. To address these concerns, the created model was validated using Leave-One-Out Cross-Validation (LOOCV), which fits the model several times using a different training and testing set each time [67]. In LOOCV, the training set consists of all but one data point, and the prediction accuracy of the model is evaluated by predicting the removed data point. This process is repeated for each data point in the data set, allowing a thorough assessment of the predictive ability of the model even with a small number of data points. Once validated, a dataset was created that contains both predicted and actual values. This data set served as the basis for calculating the key evaluation metrics: the root mean squared error (RMSE) and the mean absolute error (MAE). RMSE measures the average deviation between the predicted and actual values by calculating the square root of the average squared difference, while MAE measures the mean absolute difference between the predicted and actual values [68]. These evaluation metrics quantify the predictive performance of the model and provide valuable insights into its accuracy and reliability. The lower the MAE and RMSE, the better a model fits a data set. For easier interpretation, the predicted and actual values were visualized using a scatter plot 6.16.

6 Results of the analysis and discussion

The relationship between vegetation indices and nitrogen uptake was examined, along with other characteristics of the plants. The analysis aimed to reveal their interrelationships and correlations, which would support the possibility of using vegetation indices to estimate nitrogen uptake by plants. This chapter summarizes the results and discusses their implications. The results of the analysis are shown in Table 6.1, including the Pearson correlation coefficient and the determination coefficient.

Table 6.1: Results of the correlation and regression analysis between vegetation indices and crop characteristics. Each cell of the table contains the values of Pearson correlation coefficient and the coefficient of determination, in this order.

	NDVI	**NDRE**	**GNDVI**	**MCARI**	**EVI**
LAI	0.69, 0.47	0.53, 0.28	0.39, 0.16	0.62. 0.39	0.86, 0.74
crop height	0.43, 0.19	0.42, 0.18	0.31, 0.09	0.1, 0.01	0.33, 0.11
nitrogen concentration	-0.69, 0.48	-0.54, 0.3	-0.48, 0.23	-0.81, 0.66	-0.77, 0.6
biomass weight	0.74, 0.55	0.59, 0.35	0.51, 0.26	0.88, 0.78	0.82, 0.67
nitrogen uptake	0.86, 0.74	0.72, 0.51	0.6, 0.36	0.9, 0.81	0.95, 0.89

The results are discussed in more detail in the following subsections.

6.1 Plant nitrogen uptake of observed winter wheat

The course of nitrogen uptake changes through the observation period can be seen in the time-series plots. Figure 6.1 shows the mean nitrogen uptake for the whole field and figure 6.2 shows the mean nitrogen uptake per quadrant.

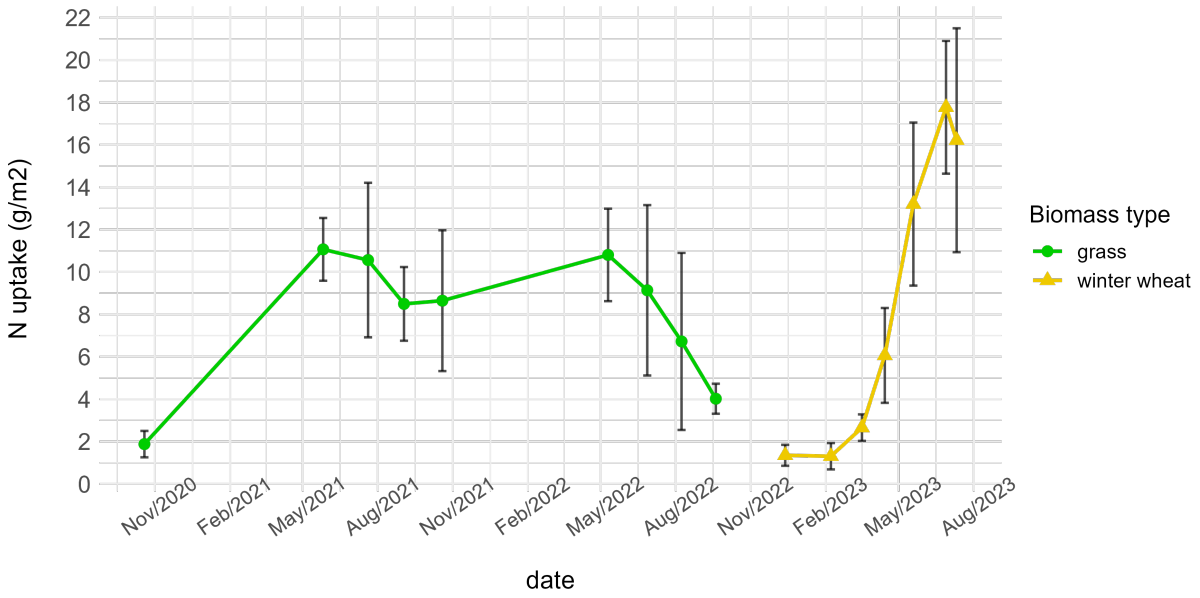

Figure 6.1: Time-series plot of mean nitrogen uptake per field in g/m^2. The biomass type is represented by color and shape of the data point. The error bars represent standard deviation.

The generated plot provides a visualization of the mean nitrogen uptake variations over the period from 19th October 2020, to 11th July 2023. The x-axis displays dates in the month/year format, while the y-axis represents nitrogen uptake in g/m^2. The plot distinguishes between the grass and the winter wheat using different shapes and colors for clarity. A line connecting the data points is present in the plot to further aid in the identification of trends over time.

Decreased nitrogen uptake in grass can be observed during September and October, which may be due to the preparation of the plants for dormancy in the upcoming winter months. This preparation can include a reduction in nutrient uptake, including nitrogen, as the grass stops growing [69]. Another reason could be the transport of nitrogen from the leaves to the roots or to storage organs within the plant, which occurs as the grass approaches the end of its growing season [70].

Cutting of the grass-clover mixture started in May 2022 with complete removal in October 2022, which is visible in the plot. The removal was followed by the sowing of winter wheat in November 2022.

In the plot, a steady increase in nitrogen uptake by winter wheat can be observed, with a decrease in July. This decrease is most likely a sign of senescence, during which nitrogen is relocated towards the grains. At this point, nitrogen uptake in the above-ground biomass is lower, although the crop remains healthy and produces high values of vegetation indices (VIs). Because of this, only measurements obtained before the end of June were included in the correlation and regression analysis between nitrogen uptake and vegetation indices.

Figure 6.2 shows the nitrogen uptake changes for each quadrant. In this plot, the quadrants are visualized in different colors and the shapes correspond to the type of biomass.

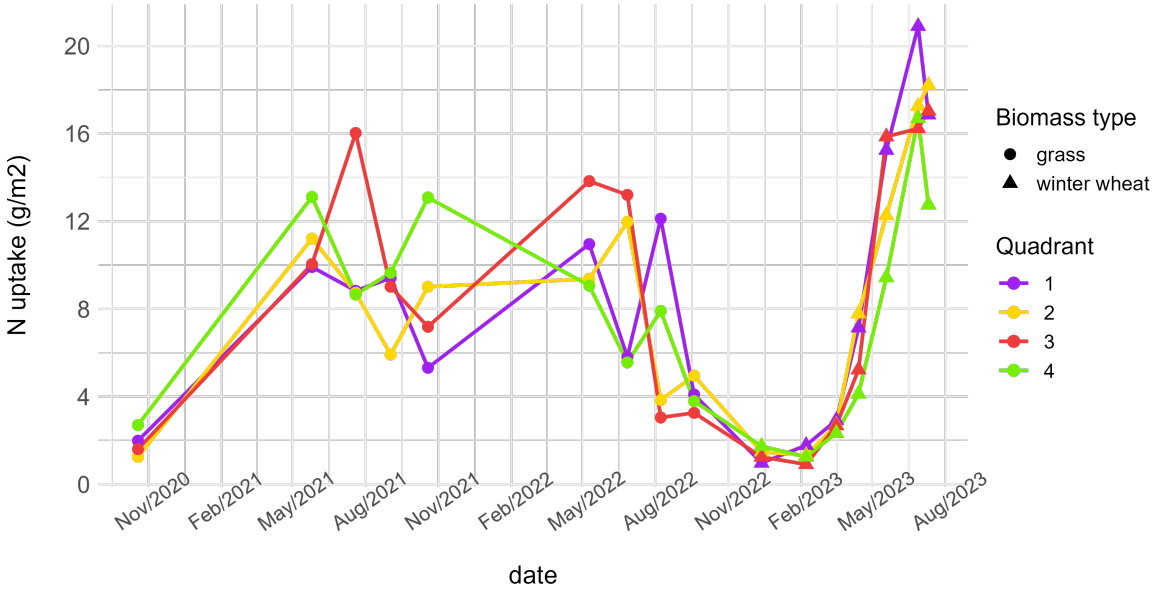

Figure 6.2: Time-series plot of nitrogen uptake per quadrants in g/m^2. The quadrants are separated by colors and the shapes represent the biomass type.

The grass cover exhibits variations in nitrogen uptake throughout the field, while nitrogen uptake of winter wheat is more consistent. Plant uptake can be affected by variability in soil conditions, moisture, pH, temperature, and other environmental factors. Variations in nitrogen uptake within grasses are likely mainly due to the nature of the mixture. Red clover (Trifolium pratense) and white clover (Trifolium repens) are nitrogen-fixing plants, which means they enrich the soil with nitrogen. Therefore, parts of the field with higher concentrations of clover would

be richer in nitrogen, and the crops collected there would exhibit higher nitrogen uptake. The age and stage of growth of the plants can also influence nitrogen uptake, with younger plants having different nutritional needs compared to mature plants. The proportions of different age groups within the samples can vary, causing further variability in nitrogen uptake.

6.2 Obtained time variations of vegetation indices

The following time-series plot 6.3 illustrates the fluctuation of the values of the Normalized Difference Vegetation Index (NDVI) over consecutive months, spanning from March 2021 to the end of June 2023. The x-axis denotes the date in a month/year format, and the y-axis represents the corresponding NDVI values, which measure the reflectance difference between near-infrared and red light. The grass cover and the winter wheat are distinguished in the plot by color and shape.

Compared to nitrogen uptake, vegetation indices offer a more detailed insight into plant dynamics due to the higher number of measurement dates. Notable decreases in NDVI values can be observed in the plot. These correspond to grass cuts, dormancy, or crop harvesting events, demonstrating the sensitivity of NDVI to changes in plant biomass and chlorophyll content.

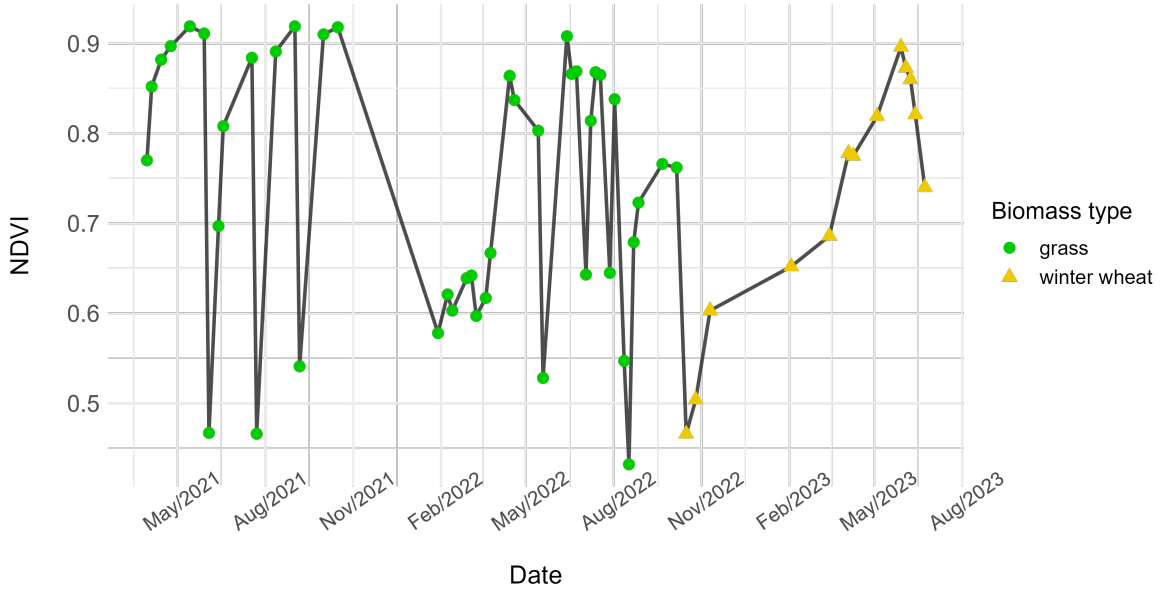

Figure 6.3: Time-series plot of NDVI for grass-clover and winter wheat over 2021-2023, highlighting changes in the status of the crops.

Low values during January, February, and March 2022 may be attributed to grass entering a dormant state due to colder temperatures and shorter daylight hours. During dormancy, grasses stop growing to conserve energy and its chlorophyll content in leaves decreases, resulting in lower NDVI values [71]. This reduction in NDVI values can be related to the decreased nitrogen uptake observed in subchapter 6.1 as lower nitrogen uptake can lead to reduced chlorophyll. However, at the moment when nitrogen uptake decreases, the grass may still appear green and healthy, which is why higher NDVI values can be observed during the fall.

Winter wheat was planted in October, after which it germinated before entering a dormant phase during the cold winter months. This limited growth period, during which winter wheat does not significantly expand its biomass, is reflected in the graph by a slow increase in NDVI

between November and March. As temperatures begin to rise in spring and daylight hours increase, winter wheat resumes active growth. This can be observed in the graph, where the NDVI values surge during the period from April to May. The peak NDVI values observed in June typically represent the maximum leaf area and chlorophyll concentration as the wheat approaches maturity. The plant then enters senescence, during which resources are diverted from leaf development towards seed maturation. Leaves begin to lose chlorophyll and die off, leading to a decrease in NDVI values around July.

On 14th May 2022, unusually low values were recorded for the vegetation indices NDVI, NDRE, and GNDVI, while MCARI and EVI showed expected levels. The indices NDRE, GNDVI, MCARI and EVI are displayed in Figure 6.4. The lower values were probably caused by rain during image acquisition, which affects the reflection of light. As depicted in Figure 2.4, water absorbs most of the light at wavelengths beyond 0.7 μm, leading to a decrease in reflectance in the near-infrared (NIR) spectrum. Healthy vegetation reflects light in the NIR spectrum and absorbs red light. The higher the reflectance in the NIR spectrum and the greater the absorption of red light, the higher the values of the Normalized Difference Vegetation Index (NDVI). However, the presence of water affects these values. Although water does not significantly change the reflectance of red light, it decreases the reflectance in the NIR spectrum, leading to lower values of the NDVI. NDRE and GNDVI are also affected in a similar way. GNDVI is most affected because water absorbs even less green light than red light. This means that there is almost no decrease in the green light reflectance, making the lower NIR reflectance have an even greater impact on the GNDVI results. Since the values were low due to weather conditions and not the actual state of the plant, the data points are not well correlated with the status of the crops and caused a lower ability of the models to predict N uptake. The deviating point is clearly visible in Figures 6.7 and 6.15.

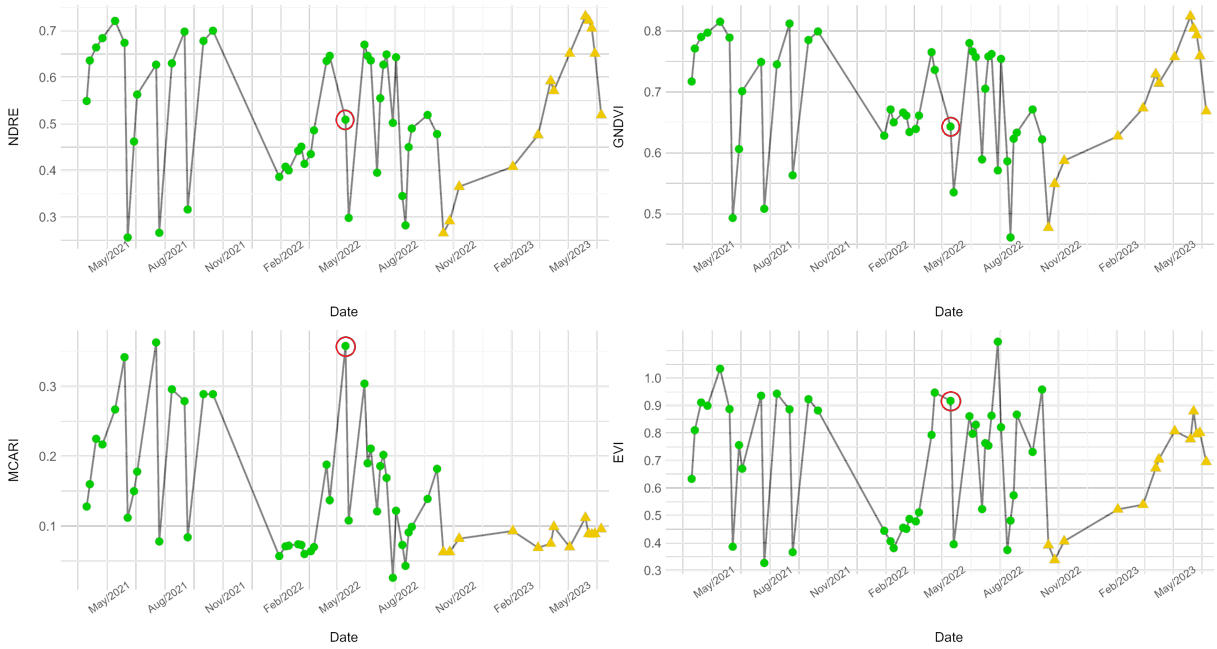

Figure 6.4: First row left to right: time-series plot of NDRE, GNDVI. Second row left to right: time-series plot of MCARI, EVI. The values from 14th May 2022 are circled. While there is a decrease in NDRE and GNDVI due to the rain, MCARI and EVI are not affected.

Indices like MCARI and EVI are less affected by rain because they are designed to minimize atmospheric and soil background influences. MCARI focuses on the red-edge spectrum, which is less affected by water reflectance, and EVI includes a blue band to correct for aerosol influences in the atmosphere.

The plot 6.5 includes the normalized values of all the observed vegetation indices to highlight their differences. Most of the indices exhibit a similar course of development, with some variations in sensitivity. In particular, MCARI stands out with its very low values for winter wheat.

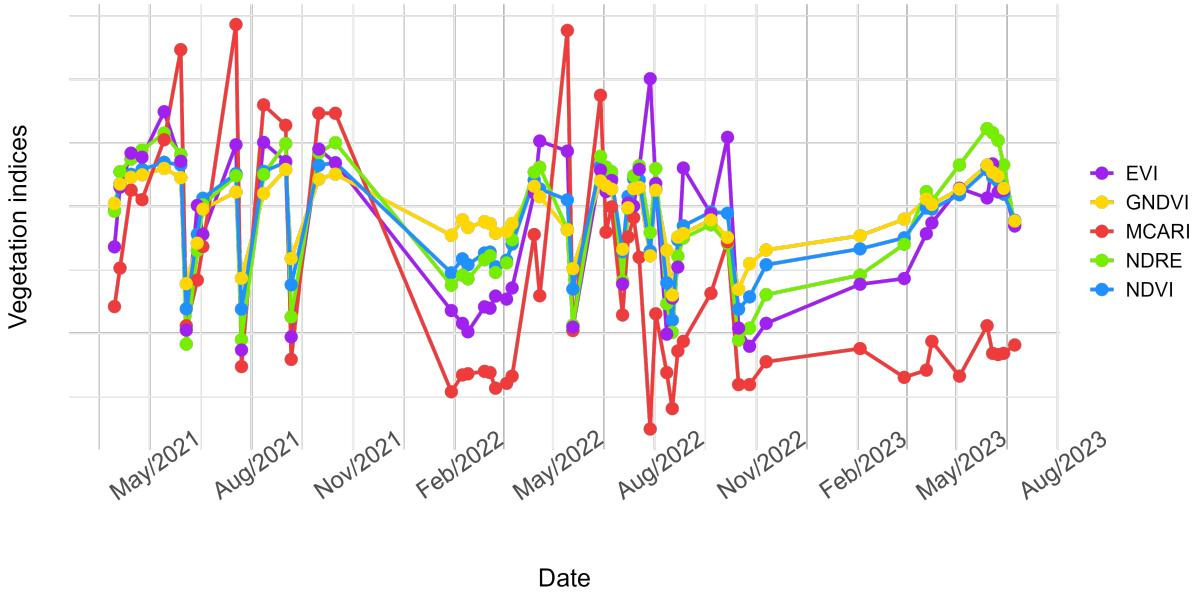

Figure 6.5: Time-series plot of all the observed vegetation indices to highlight their differences. The values are normalized.

Time series of vegetation indices were also collected per quadrant. However, because of the low spatial resolution of the images, each quadrant consisted of only a few large pixels. These pixels often overlapped with the boundaries of the quadrants, resulting in unreliable values. Consequently, minimal variations in vegetation indices were observed between the different quadrants.

6.3 Results of correlation and regression analysis

The relationship between vegetation indices (VIs) and Leaf Area Index (LAI), crop height, dry biomass weight, nitrogen concentration, and nitrogen uptake was analyzed. The results of each correlation and regression analysis were visualized in scatterplots that include the correlation coefficient and the coefficient of determination.

Relationship between VIs and Leaf Area Index (LAI)

Among the vegetation indices analyzed, the Enhanced Vegetation Index (EVI) showed the strongest relationship with LAI, with R^2=0.74 and r=0.86. The high correlation coefficient suggests a strong positive relationship, meaning that as LAI increases, EVI also tends to increase. The R^2 value indicates that 74% of the variability in LAI can be explained by the variability in EVI.

In contrast, the Green Normalized Difference Vegetation Index (GNDVI) showed a much weaker relationship with R^2=0.16 and r=0.39. This implies that only 16% of the variation in LAI can be explained by changes in GNDVI. In this case, the low correlation is mainly due to the inability of GNDVI to correct for the influence of the atmospheric and soil background. One point can be seen in the scatterplot that is deviating greatly from the line of best fit and is causing the inaccuracy of the model. This point represents the GNDVI value obtained on 14th May 2022 and is most likely lower than the real value due to the influence of rain on the reflectance.

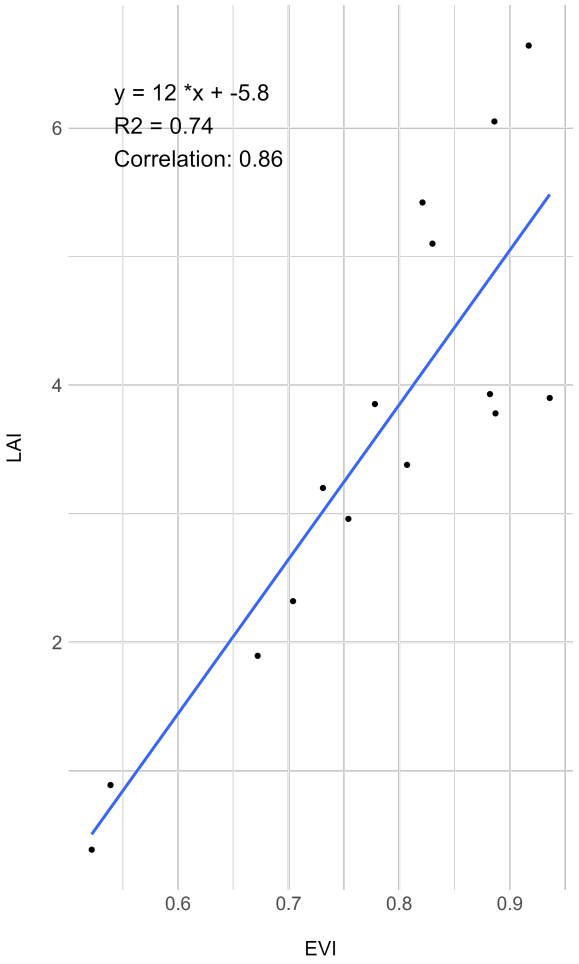

Figure 6.6: Relationship between EVI and LAI.

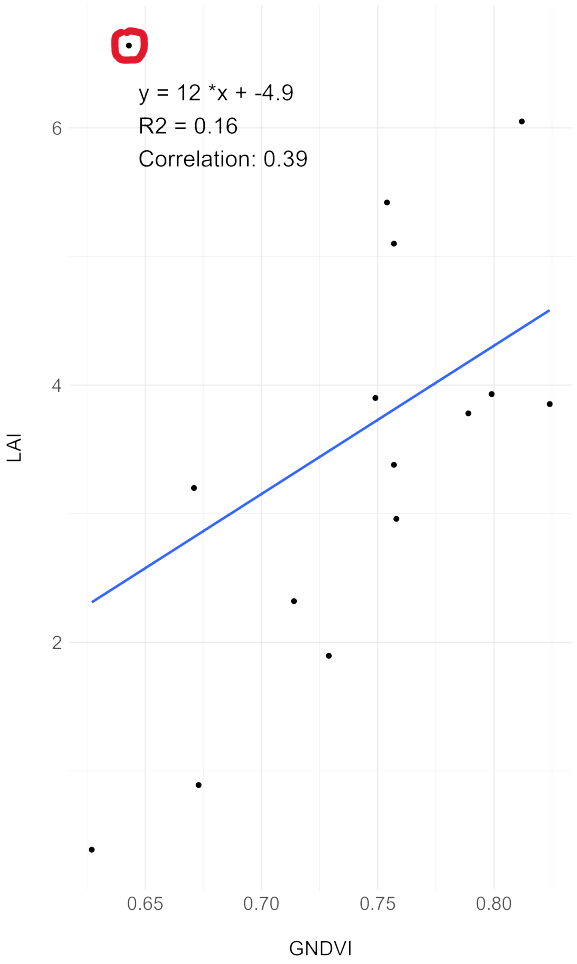

Figure 6.7: Relationship between GNDVI and LAI. A data point that is influenced by atmospheric noise is highlighted in red.

Relationship between VIs and crop height

Crop height was not highly correlated with any of the indices analyzed. This was expected as vegetation indices reflect aspects of crop health and physiological status. Crop height does not necessarily relate to these factors because tall crops can be unhealthy or sparse, and shorter crops can be dense and vigorous.

Crop height was most strongly correlated with NDVI, but even then an R^2 of only 0.19 and a correlation coefficient of 0.43 were achieved. This could be due to the fact that NDVI captures the overall biomass, which coincidentally correlates with crop height, as higher crops usually have more biomass.

The lowest correlation was observed with the Modified Chlorophyll Absorption Ratio Index (MCARI), with a very low R^2 of 0.01 and a correlation coefficient (r) of 0.1, which means that there is basically no relationship between MCARI and crop height. Since MCARI was designed to serve as an indicator of chlorophyll concentration, it is insensitive to variations in height, which do not directly affect chlorophyll content.

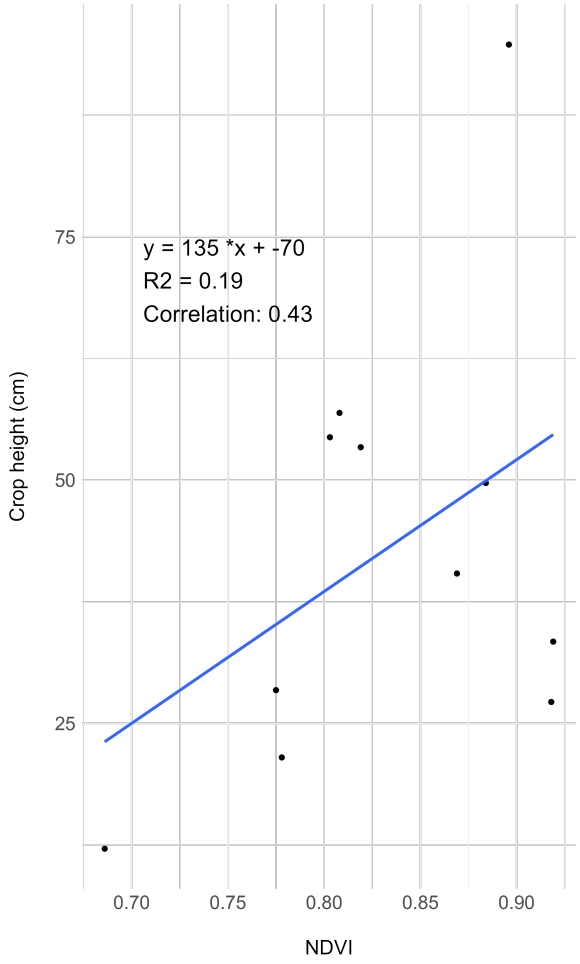

Figure 6.8: Relationship between NDVI and crop height.

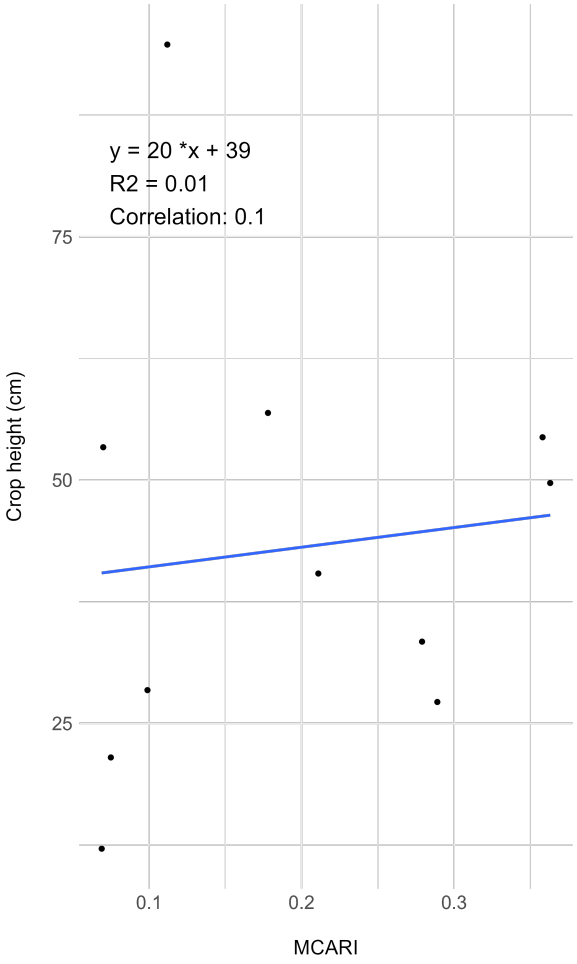

Figure 6.9: Relationship between MCARI and crop height.

Relationship between VIs and nitrogen concentration

The correlation between vegetation indices and nitrogen concentration was negative, which means that as the VI values increase, the nitrogen concentration decreases. This inverse relationship can be attributed to the so-called dilution effect, a phenomenon in which the accumulation of dry biomass is accompanied by a decrease in the concentration of nutrients in plant tissues. This is because when the crop intakes a growth-limiting elements, such as nitrogen, the dry biomass accumulates more rapidly than the amount of nitrogen [72]. As a result, although the total amount of nitrogen has grown, its concentration relative to the biomass has decreased.

Among the indices analyzed, MCARI exhibited the strongest negative correlation with nitrogen concentration, with R^2=0.66 and r=-0.81. The good results can be attributed to the fact that MCARI is designed to observe the chlorophyll content of the leaf, which is closely related to the nitrogen content.

On the other hand, GNDVI showed the weakest correlation across the indices, with R^2=0.23 and r=-0.48, indicating a lower sensitivity to changes in nitrogen concentration within plant tissues. The measurement point from May 2022 was not as deviated during this analysis as it was with LAI.

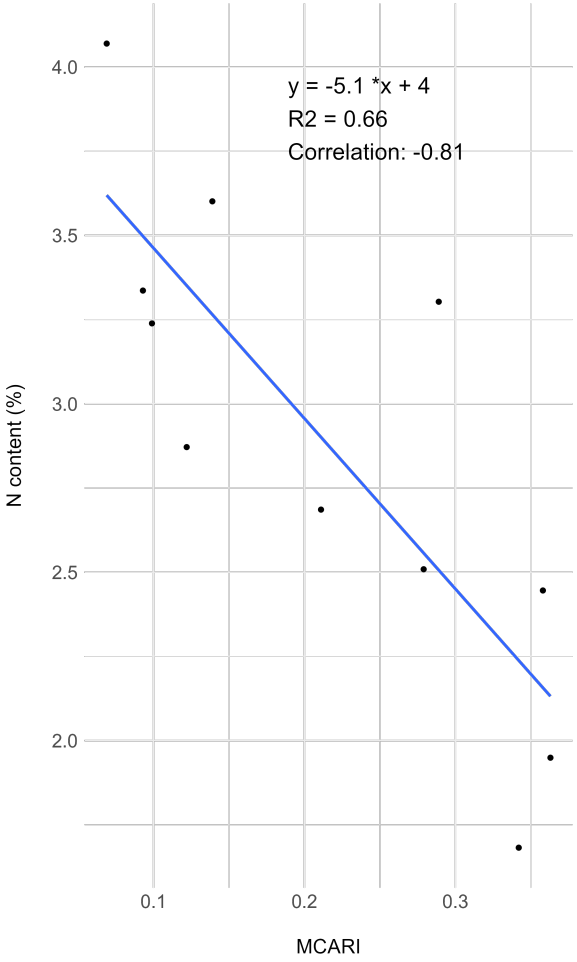

Figure 6.10: Relationship between MCARI and nitrogen concentration in the above ground biomass.

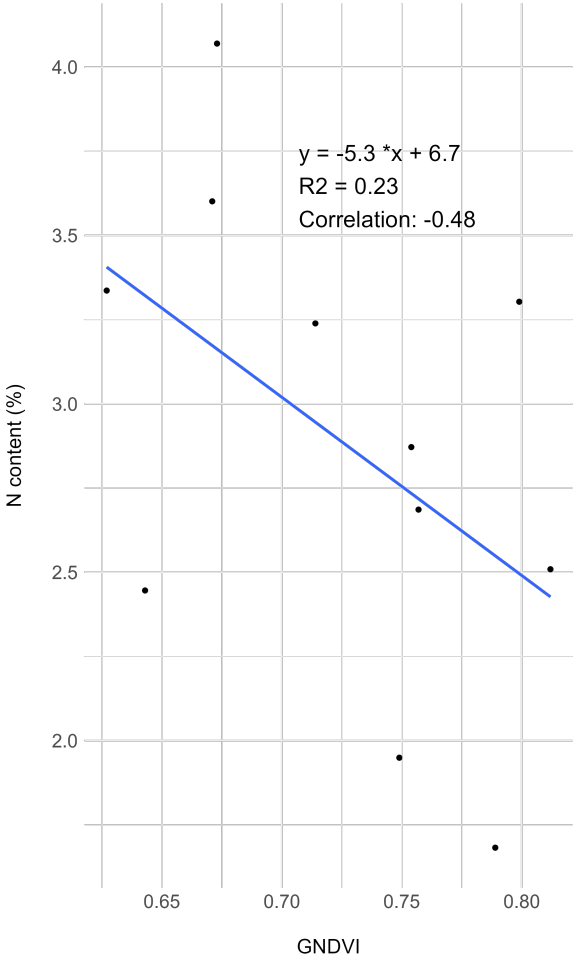

Figure 6.11: Relationship between GNDVI and nitrogen concentration in the above ground biomass.

Relationship between VIs and biomass weight

Similarly to nitrogen concentration, the most well correlated index with biomass weight was MCARI and the least correlated index was GNDVI. MCARI resulted in R^2=0.78 and r=0.88, while for GNDVI R^2=0.26 and r=0.51. As mentioned above, MCARI is sensitive to leaf chlorophyll, which usually increases together with biomass; therefore, MCARI is also capable of effectively capturing the biomass weight of crops.

GNDVI exhibited a much weaker correlation, with an R^2=0.26 and r=0.51. Interestingly, GNDVI showed a good correlation at lower biomass weight values, but the correlation weakened when the biomass weight exceeded 40 grams. The correlation at lower biomass weights is clearly visible in Figure 6.13 where the values below 40 g appear to increase linearly with GNDVI. This suggests that GNDVI is more effective in monitoring sparse vegetation as it becomes oversaturated with denser canopies. Dense canopies absorb and scatter more green light, which is then not being reflected and captured by the index. As a result, GNDVI remains the same even though the biomass weight continues to increase.

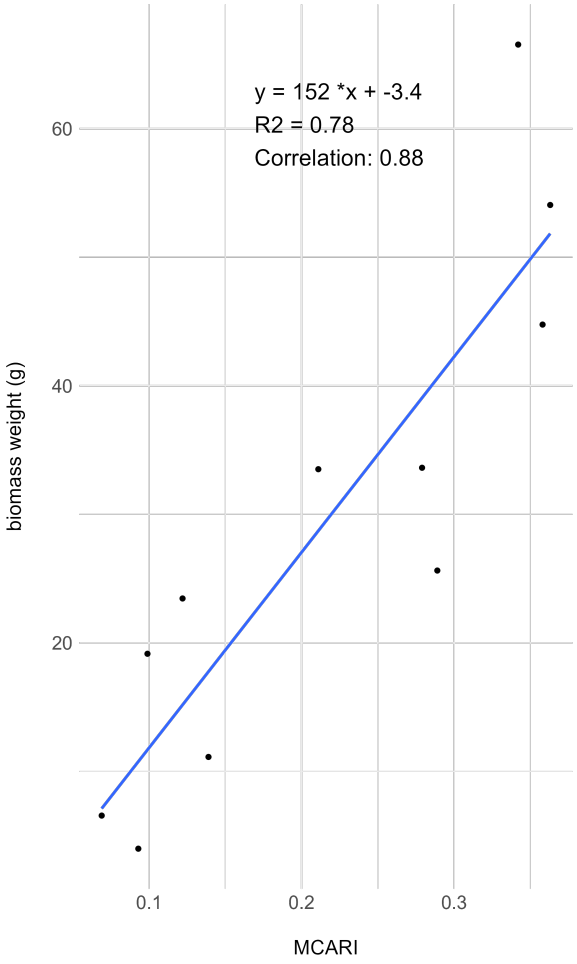

Figure 6.12: Relationship between MCARI and biomass weight.

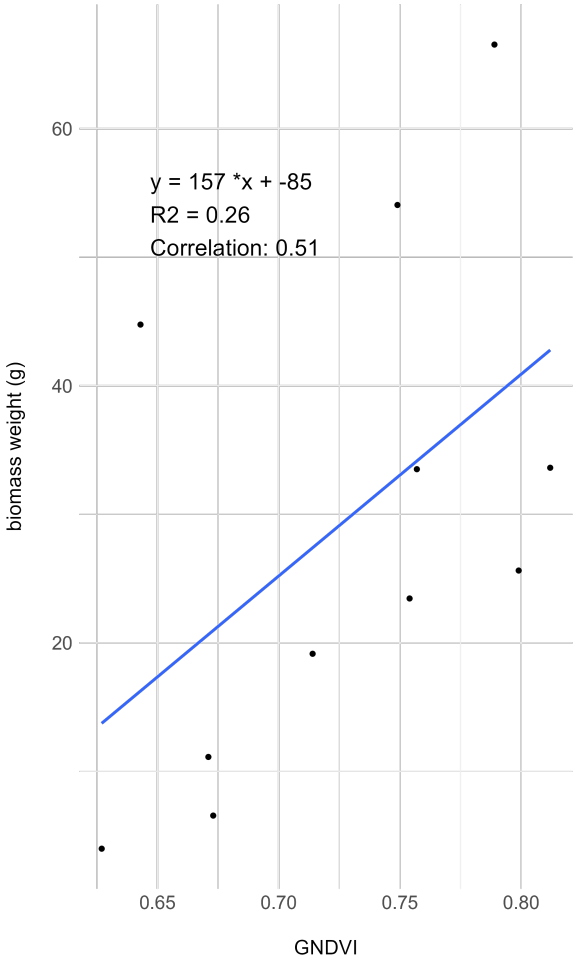

Figure 6.13: Relationship between GNDVI and biomass weight. Positive correlation can be observed for biomass weight below 40 g, while higher values do not seem to have a strong relationship with GNDVI.

Relationship between VIs and nitrogen uptake

Significant differences in indices performance were observed during correlation and regression analysis between vegetation indices and nitrogen uptake.

EVI exhibited the strongest relationship with nitrogen uptake, achieving an R^2 of 0.89 and a correlation coefficient (r) of 0.95. This indicates that EVI is highly effective in predicting nitrogen uptake, likely due to its sensitivity to changes in chlorophyll content and canopy structure, and its ability to correct for atmospheric and soil interference. The relationship between EVI and nitrogen uptake is plotted in Figure 6.14. Since EVI showed the highest correlation and predictive capacity with nitrogen uptake, it was later used in the prediction model.

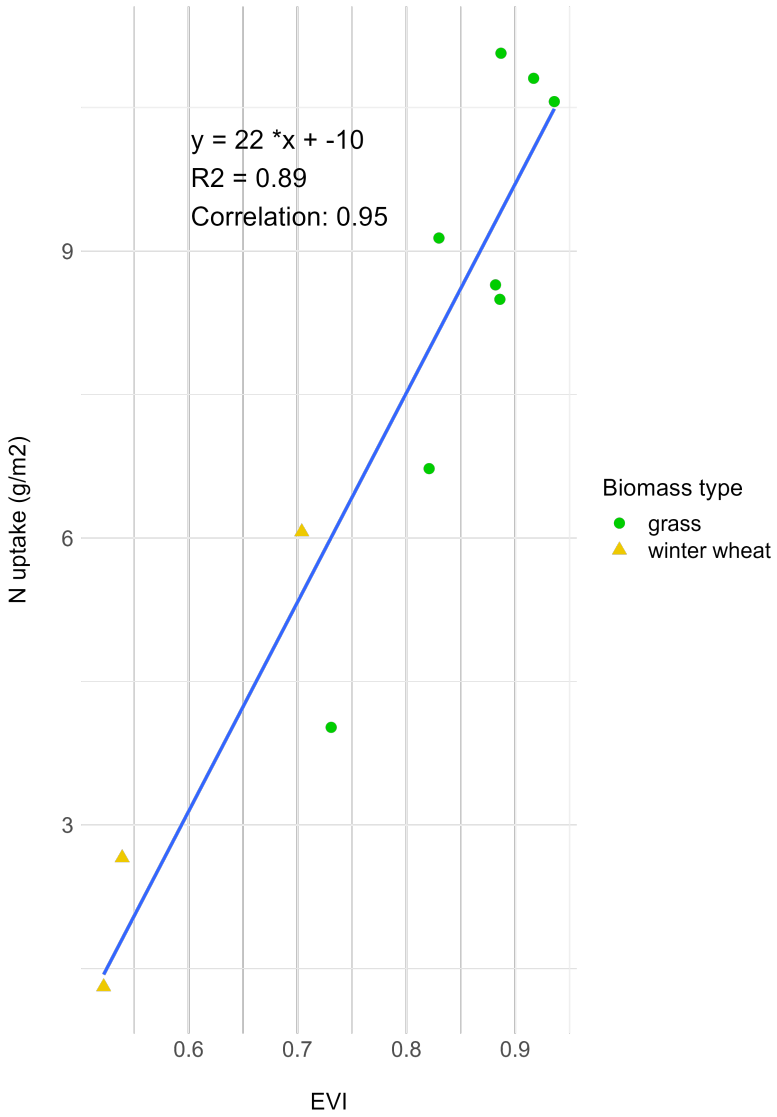

Figure 6.14: Relationship between EVI and N uptake.

In contrast, the Green Normalized Difference Vegetation Index (GNDVI) showed much weaker results, with an R^2 of only 0.36 and a correlation coefficient of 0.6. This relatively low correlation can be attributed primarily to the inability of GNDVI to correct for atmospheric influence. The GNDVI value from May 2022, which was lower than the real value due to rain, significantly affected the accuracy of the model and caused the low R^2 and the correlation coefficient. The relationship between GNDVI and nitrogen uptake can be seen in Figure 6.15.

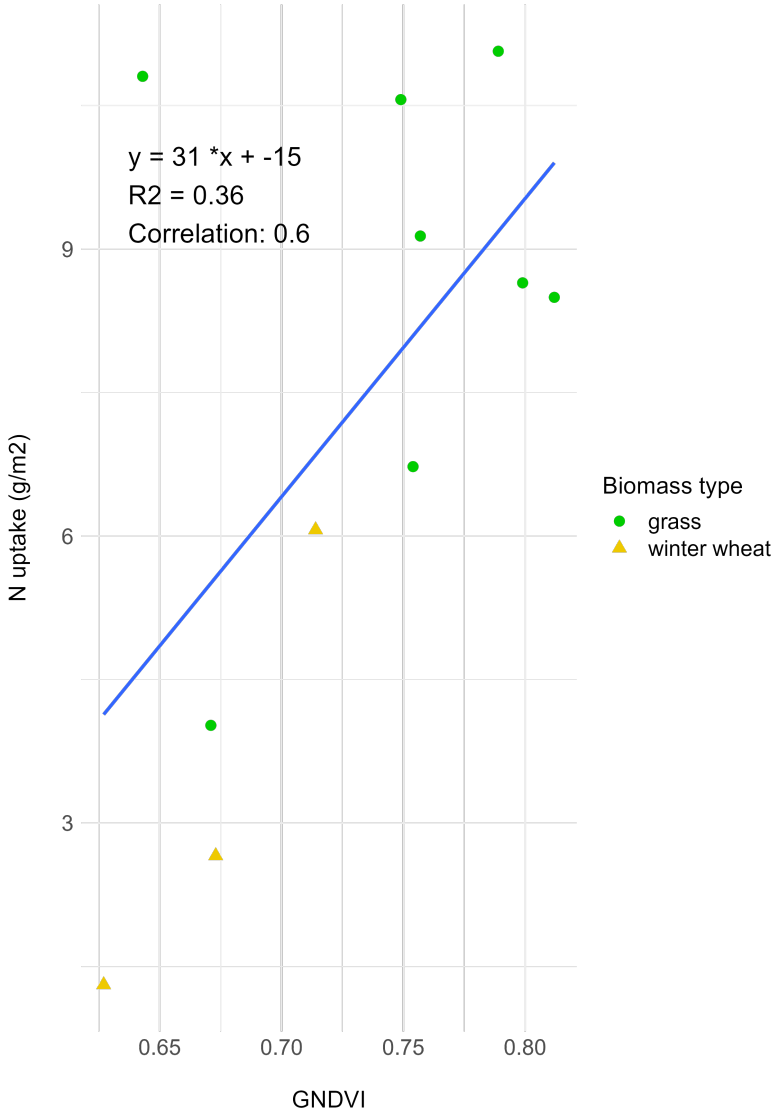

Figure 6.15: Relationship between GNDVI and N uptake. Measurement point influenced by rain is clearly deviating from the rest of the values. This point is located in the top left corner.

It is notable that while MCARI performed better in the correlation and regression analysis with nitrogen concentration and biomass weight, EVI showed a stronger relationship with nitrogen uptake. This is likely because factors such as environmental stressors or management practices can cause fluctuations in nitrogen uptake but do not immediately affect chrolophyll levels in leaves, which MCARI measures. Therefore, MCARI cannot capture these changes.

6.4 Prediction model performance

The Enhanced Vegetation Index (EVI) was used to create the prediction model, because it performed the best during the correlation and regression analysis between the indices and nitrogen uptake.

The prediction model was evaluated using the LOOCV method, which was chosen due to the limited number of data points. This method ensures that each data point is used for both training and validation, thus maximizing the use of available data and avoiding overfitting.

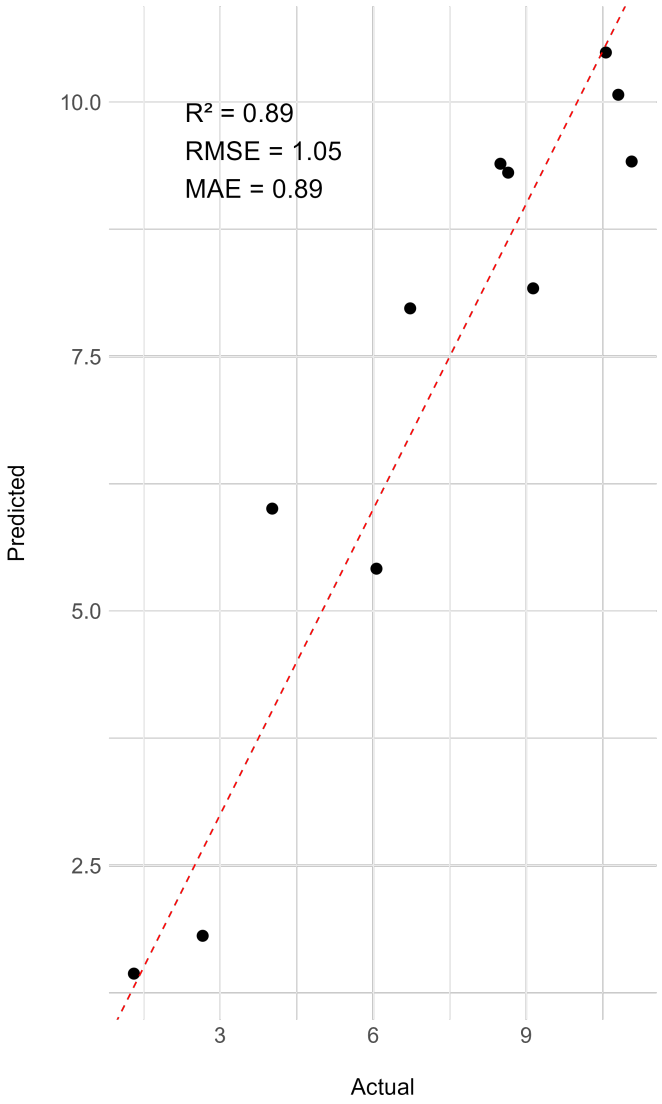

Figure 6.16: The N uptake predicted by EVI plotted against the real data. The 1:1 line represents a condition where predicted values exactly match the real values.

The model achieved an R^2 of 0.89, indicating a high level of accuracy in the predictions compared to the actual values of nitrogen uptake. The precision of the model was further quantified by calculating the Root Mean Square Error (RMSE) and the Mean Absolute Error (MAE), with values of 1.05 and 0.89, respectively. An RMSE of 1.05 means that the square root of the average squared differences between the predicted values made by the model and the actual values is 1.05 units (in this case g/m^2). Similarly, an MAE of 0.89 means that, on

average, the the predicted values are 0.89 units away from the actual data points. Although both RMSE and MAE provide measures of average error, RMSE gives a relatively higher weight to larger errors, which can reveal the sensitivity of the model to outliers. The relationship between predicted and real values was visualized in Figure 6.16.

In the scatter plot, the points are arranged along a so-called 1:1 line, which represents a perfect condition, where the predicted values exactly match the actual values. The points are distributed closely around the line, which indicates accurate and consistent predictions of the model and confirms the suitability of EVI as a predictive tool for nitrogen uptake.

In conclusion, high R^2, low RMSE, and MAE confirm the effectiveness of the EVI-based model in accurately predicting nitrogen uptake.

6.5 Comparison with existing literature

The methodology of this study differed from other research in several ways. First, data collection was restricted to a short period of time and was performed at only one field site. This limited the number of observations, potentially affecting the robustness and generalizability of the results. Secondly, while most studies focus on a single crop, in this thesis both grass and winter wheat were analyzed simultaneously. The results suggested that some indices were effective for both crops, while others were more crop specific. For example, MCARI appeared to perform rather well when analyzing its relationship with grass nitrogen uptake ($r=0.88$, $R^2=0.78$), but there did not seem to be a strong relationship between MCARI and nitrogen uptake of winter wheat ($r=0.42$, $R^2=0.18$). However, this could be caused by the low number of nitrogen uptake measurements of winter wheat. Other studies found that there is a non-linear relationship between MCARI and chlorophyll leave content in winter wheat [73], which would also explain the low performance.

EVI was the best-performing vegetation index; however, it did not perform as well in other studies, such as the one conducted by Troy et al. [74], where NDRE outperformed EVI. This could indicate that, while EVI does not perform well when analyzing winter wheat by itself, it yields better results when both grass and winter wheat, or only grass, are observed. The method of acquisition of satellite images could also play a role. The study by Troy et al. only included satellite images captured at the peak of greenness in the calculation, while in this study images from across the entire crop life cycle were used. NDRE also performed well in this study but was limited by its inability to correct for atmospheric influence.

In contrast to the previous literature, GNDVI showed the lowest performance in predicting nitrogen uptake in this study. This was unexpected, as GNDVI is generally considered to be more sensitive to chlorophyll concentrations and nitrogen uptake in crops compared to other indices such as NDVI. For example, Francisco et al. [75] demonstrated high efficiency of GNDVI under controlled greenhouse conditions with crops such as cucumbers and broccoli. Similarly, studies that analyzed corn yield [76] using spectral images collected from an aircraft have found strong correlations between GNDVI and nitrogen uptake. It is important to note that in both cases the atmospheric influences were negligible because of the nature of image acquisition and field characteristics. These findings suggest that while GNDVI can be a reliable indicator under controlled conditions, it may not perform well under field conditions with atmospheric variability. Other studies in which vegetation indices were calculated from satellite images confirmed the results of this work [44].

Currently, most studies use vegetation indices only on one crop at a time. Future research should investigate the development and validation of vegetation indices that are reliable for multiple types of crops, which would have practical implications for agricultural management.

7 Conclusion

In summary, this thesis investigated the relationships between vegetation indices and nitrogen uptake, along with other plant characteristics, using correlation and regression analysis. In addition, a model was developed to predict nitrogen uptake based on the Enhanced Vegetation Index (EVI).

Time-series analysis revealed different nitrogen uptake patterns in grass and winter wheat, reflecting different environmental and physiological factors. In particular, the time-series plots of the vegetation indices highlighted various changes in crop status throughout its life cycle.

Correlation and regression analyzes were performed to better understand the relationship between vegetation indices and nitrogen uptake together with other vegetation characteristics. EVI showed a strong correlation with the Leaf Area Index (LAI) and nitrogen uptake. Nitrogen concentration and biomass weight were best correlated with the Modified Chlorophyll Absorption in Reflectance Index (MCARI), while crop height was not strongly correlated with any of the indices. In contrast to other studies, the Green Normalized Difference Vegetation Index (GNDVI) did not perform well, mainly due to its sensitivity to atmospheric conditions, which caused a lower value for a speficic date.

A prediction model was created that uses EVI to predict nitrogen uptake. It achieved very good results, with an R^2 of 0.89, an RMSE of 1.05, and an MAE of 0.89. This indicates that EVI is suitable for predicting nitrogen uptake in grass and winter wheat. This model could be used in precision agriculture, allowing monitoring and optimizing nitrogen application. However, it should be tested under various climatic conditions and for different crop species to validate its applicability and robustness.

There were many limitations in the performed analysis. The main limitation was the insufficient number of manual measurements, particularly for winter wheat, which had only three measurement points. This is not enough to confidently conclude the relationship between nitrogen uptake of winter wheat and vegetation indices. Even when grass data were included in the dataset, there were only 11 data points in total. To improve the results, more nitrogen uptake measurements are necessary. Another drawback was that the satellite images were only taken once per five days and as a result the vegetation indices values could not be precisely combined with nitrogen uptake. Cloud cover further complicated the analysis, as images taken on cloudy days are unreliable and had to be excluded. The removal of cloud-covered images greatly reduced the final number of vegetation index values. Therefore, vegetation indices derived from satellite images have a greater potential for use in regions with low cloud cover.

The results of this thesis contribute to the understanding of the relationship between vegetation indices and crop characteristics, particularly nitrogen uptake. This can help significantly mitigate the negative impacts of excessive fertilization, including environmental pollution and economic loss. Better fertilization practices would reduce nutrient runoff, water pollution, greenhouse gas emissions, and unnecessary economic costs. The Enhanced Vegetation Index (EVI) showed a strong ability to predict nitrogen uptake by crops, making it a useful tool for adjusting fertilizer application to the actual needs of crops.

Bibliography

[1] Harrison, P. J. A. The Nitrogen Cycle. *Visionlearning*. 2003, EAS-2 (4).

[2] Ladha, J. K., Pathak, H., Krupnik, T. J., Six, J. and Kessel, C. van. Efficiency of Fertilizer Nitrogen in Cereal Production: Retrospects and Prospects. In:. 2005, p. 85–156. DOI: 10.1016/S0065-2113(05)87003-8.

[3] Vitousek, P. M., Aber, J. D., Howarth, R. W., Likens, G. E., Matson, P. A. et al. HUMAN ALTERATION OF THE GLOBAL NITROGEN CYCLE: SOURCES AND CONSEQUENCES. *Ecological Applications*. 1997, vol. 7, no. 3, p. 737–750. DOI: https://doi.org/10.1890/1051-0761(1997)007[0737:HAOTGN]2.0.CO;2. Available at: https://esajournals.onlinelibrary.wiley.com/doi/abs/10.1890/1051-0761%281997%29007%5B0737%3AHAOTGN%5D2.0.CO%3B2.

[4] Epa, U. and Division, C. C. *Inventory of U.S. Greenhouse Gas Emissions and Sinks: 1990-2019 – Main Text - Corrected Per Corrigenda, Updated 05/2021*. 2019. Available at: https://www.epa.gov/ghgemissions/inventory-us-greenhouse-gas-emissions-and-sinks.

[5] Food and United Nations, A. O. of the. *The international Code of Conduct for the sustainable use and management of fertilizers*. 2009.

[6] Piikki, K., Söderström, M. and Stadig, H. Remote sensing and on-farm experiments for determining in-season nitrogen rates in winter wheat – Options for implementation, model accuracy and remaining challenges. *Field Crops Research*. december 2022, vol. 289, p. 108742. DOI: 10.1016/j.fcr.2022.108742. ISSN 03784290.

[7] Miao, Y., Khosla, R. and Mulla, D. J. *Remote Sensing for Precision Nitrogen Management*. 2022. Available at: www.mdpi.com/journal/remotesensing.

[8] Basso, B., Cammarano, D., Grace, P. R., Cafiero, G., Sartori, L. et al. Criteria for Selecting Optimal Nitrogen Fertilizer Rates for Precision Agriculture. *Italian Journal of Agronomy*. Dec. 2009, vol. 4, no. 4, p. 147–158. DOI: 10.4081/ija.2009.4.147. Available at: https://agronomy.it/index.php/agro/article/view/ija.2009.4.147.

[9] Galloway, J. N., Aber, J. D., Erisman, J. W., Seitzinger, S. P., Howarth, R. W. et al. The Nitrogen Cascade. *BioScience*. april 2003, vol. 53, no. 4, p. 341–356. DOI: 10.1641/0006-3568(2003)053[0341:TNC]2.0.CO;2. ISSN 0006-3568. Available at: https://doi.org/10.1641/0006-3568(2003)053[0341:TNC]2.0.CO;2.

[10] Fowler, D., Coyle, M., Skiba, U., Sutton, M. A., Cape, J. N. et al. The global nitrogen cycle in the twenty-first century. *Philos Trans R Soc Lond B Biol Sci*. 2013, vol. 368, no. 1621, p. 20130164. DOI: 10.1098/rstb.2013.0164.

[11] Widdison, P. and Burt, T. Nitrogen Cycle. In: Jørgensen, S. E. and Fath, B. D., ed. *Encyclopedia of Ecology*. Oxford: Academic Press, 2008, p. 2526–2533. DOI: https://doi.org/10.1016/B978-008045405-4.00750-3. ISBN 978-0-08-045405-4. Available at: https://www.sciencedirect.com/science/article/pii/B9780080454054007503.

[12] Rascio, N. and La Rocca, N. Biological Nitrogen Fixation. In: Jørgensen, S. E. and Fath, B. D., ed. *Encyclopedia of Ecology*. Oxford: Academic Press, 2008, p. 412–419. DOI: https://doi.org/10.1016/B978-008045405-4.00273-1. ISBN 978-0-08-045405-4. Available at: https://www.sciencedirect.com/science/article/pii/B9780080454054002731.

[13] Newton, W. E. Chapter 8 - Physiology, Biochemistry, and Molecular Biology of Nitrogen Fixation. In: Bothe, H., Ferguson, S. J. and Newton, W. E., ed. *Biology of the Nitrogen Cycle*. Amsterdam: Elsevier, 2007, p. 109–129. DOI: https://doi.org/10.1016/B978-044452857-5.50009-6. ISBN 978-0-444-52857-5. Available at: https://www.sciencedirect.com/science/article/pii/B9780444528575500096.

[14] Strock, J. Ammonification. In: Jørgensen, S. E. and Fath, B. D., ed. *Encyclopedia of Ecology*. Oxford: Academic Press, 2008, p. 162–165. DOI: https://doi.org/10.1016/B978-008045405-4.00256-1. ISBN 978-0-08-045405-4. Available at: https://www.sciencedirect.com/science/article/pii/B9780080454054002561.

[15] Ward, B. Nitrification. In: Jørgensen, S. E. and Fath, B. D., ed. *Encyclopedia of Ecology*. Oxford: Academic Press, 2008, p. 2511–2518. DOI: https://doi.org/10.1016/B978-008045405-4.00280-9. ISBN 978-0-08-045405-4. Available at: https://www.sciencedirect.com/science/article/pii/B9780080454054002809.

[16] Tischner, R. and Kaiser, W. Chapter 18 - Nitrate Assimilation in Plants. In: Bothe, H., Ferguson, S. J. and Newton, W. E., ed. *Biology of the Nitrogen Cycle*. Amsterdam: Elsevier, 2007, p. 283–301. DOI: https://doi.org/10.1016/B978-044452857-5.50019-9. ISBN 978-0-444-52857-5. Available at: https://www.sciencedirect.com/science/article/pii/B9780444528575500199.

[17] Masclaux Daubresse, C., Daniel Vedele, F., Dechorgnat, J., Chardon, F., Gaufichon, L. et al. Nitrogen uptake, assimilation and remobilization in plants: Challenges for sustainable and productive agriculture. *Annals of botany*. march 2010, vol. 105, p. 1141–57. DOI: 10.1093/aob/mcq028.

[18] Wen, B., Li, C., Fu, X., Li, D., Li, L. et al. Effects of nitrate deficiency on nitrate assimilation and chlorophyll synthesis of detached apple leaves. *Plant Physiology and Biochemistry*. 2019, vol. 142, p. 363–371. DOI: https://doi.org/10.1016/j.plaphy.2019.07.007. ISSN 0981-9428. Available at: https://www.sciencedirect.com/science/article/pii/S0981942819302864.

[19] van Spanning, R. J., Richardson, D. J. and Ferguson, S. J. Chapter 1 - Introduction to the Biochemistry and Molecular Biology of Denitrification. In: Bothe, H., Ferguson, S. J. and Newton, W. E., ed. *Biology of the Nitrogen Cycle*. Amsterdam: Elsevier, 2007, p. 3–20. DOI: https://doi.org/10.1016/B978-044452857-5.50002-3. ISBN 978-0-444-52857-5. Available at: https://www.sciencedirect.com/science/article/pii/B9780444528575500023.

[20] Skiba, U. Denitrification. In: Jørgensen, S. E. and Fath, B. D., ed. *Encyclopedia of Ecology*. Oxford: Academic Press, 2008, p. 866–871. DOI: https://doi.org/10.1016/B978-008045405-4.00264-0. ISBN 978-0-08-045405-4. Available at: https://www.sciencedirect.com/science/article/pii/B9780080454054002640.

[21] Charles Munch, J. and Velthof, G. L. Chapter 21 - Denitrification and Agriculture. In: Bothe, H., Ferguson, S. J. and Newton, W. E., ed. *Biology of the Nitrogen Cycle*. Amsterdam: Elsevier, 2007, p. 331–341. DOI: https://doi.org/10.1016/B978-044452857-5.50022-9. ISBN 978-0-444-52857-5. Available at: https://www.sciencedirect.com/science/article/pii/B9780444528575500229.

[22] Jamali, H., Quayle, W. C., Scheer, C., Rowlings, D. W. and Baldock, J. A. Effect of soil texture and wheat plants on N2O fluxes: A lysimeter study. *Agricultural and Forest Meteorology*. 2016, vol. 223, p. 17–29. Available at: https://api.semanticscholar.org/CorpusID:87924091.

[23] Camp, H. J. O. den, Jetten, M. S. and Strous, M. Anammox. In:. Elsevier, 2007, p. 245–262. DOI: 10.1016/B978-044452857-5.50017-5. Available at: https://linkinghub.elsevier.com/retrieve/pii/B9780444528575500175.

[24] Galloway, J., Dentener, F. and Capone, e. a. Nitrogen Cycles: Past, Present, and Future. *Biogeochemistry*. 2004, vol. 70, p. 153–226. DOI: 10.1007/s10533-004-0370-0. Available at: https://doi.org/10.1007/s10533-004-0370-0.

[25] Centre, S. R. *Planetary boundaries*. Accessed: Nov. 16, 2023. [Online]. Available at: https://www.stockholmresilience.org/research/planetary-boundaries.html.

[26] Galloway, J. N., Bleeker, A. and Erisman, J. W. The Human Creation and Use of Reactive Nitrogen: A Global and Regional Perspective. *Annual Review of Environment and Resources*. 2021, vol. 46, no. 1, p. 255–288. DOI: 10.1146/annurev-environ-012420-045120. Available at: https://doi.org/10.1146/annurev-environ-012420-045120.

[27] Erisman, J. W., Galloway, J. N., Seitzinger, S., Bleeker, A., Dise, N. B. et al. Consequences of Human Modification of the Global Nitrogen Cycle. *Phil. Trans. R. Soc. B*. 2013, vol. 368, p. 20130116. DOI: 10.1098/rstb.2013.0116. Available at: http://doi.org/10.1098/rstb.2013.0116.

[28] Padilla, F. M., Gallardo, M. and Manzano Agugliaro, F. Global trends in nitrate leaching research in the 1960–2017 period. *Science of The Total Environment*. 2018, vol. 643, p. 400–413. DOI: https://doi.org/10.1016/j.scitotenv.2018.06.215. ISSN 0048-9697. Available at: https://www.sciencedirect.com/science/article/pii/S0048969718322915.

[29] Bruthans, J., Kůrková, I. and Kadlecová, R. Factors controlling nitrate concentration in space and time in wells distributed along an aquifer/river interface (Káraný, Czechia). *Hydrogeol J*. 2019, vol. 27, p. 195–210. DOI: 10.1007/s10040-018-1854-7. Available at: https://doi.org/10.1007/s10040-018-1854-7.

[30] Fowler, D., Coyle, M., Skiba, U., Sutton, M. A., Cape, J. N. et al. The global nitrogen cycle in the twenty-first century. *Philosophical transactions of the Royal Society of London. Series B, Biological sciences*. 2013, vol. 368, no. 1621, p. 20130164. DOI: 10.1098/rstb.2013.0164.

[31] Žížala, D., Lukas, V. and Kumhálová, J. *DÁLKOVÝ PRŮZKUM ZEMĚ A PRECIZNÍ ZEMĚDĚLSTVÍ* [Zemědělský svaz ČR - Česká technologická platforma pro zemědělství]. 2021. Accessed: December 20, 2023. Available at: http://www.slpk.sk/eldo/2022/misc/ctpz/dalkovy-pruzkum.pdf.

[32] Stafford, J. V. Implementing Precision Agriculture in the 21st Century. *Journal of Agricultural Engineering Research*. 2000, vol. 76, no. 3, p. 267–275. DOI: https://doi.org/10.1006/jaer.2000.0577. ISSN 0021-8634. Available at: https://www.sciencedirect.com/science/article/pii/S0021863400905778.

[33] Schowengerdt, R. A. *Remote Sensing: Models and Methods for Image Processing*. Boston: Academic Press, 2007. ISBN 9780123694072.

[34] Zhuge, X., Zou, X. and Wang, Y. A Fast Cloud Detection Algorithm Applicable to Monitoring and Nowcasting of Daytime Cloud Systems. *IEEE Transactions on Geoscience and Remote Sensing*. november 2017, vol. 55, p. 6111–6119. DOI: 10.1109/TGRS.2017.2720664.

[35] Petropoulos, G. P. and Kalaitzidis, C. MULTISPECTRAL VEGETATION INDICES IN REMOTE SENSING: AN OVERVIEW. In: Zhang, W., ed. *Ecological Modeling*. 75, Iera Odos St., Athens, Greece: Nova Science Publishers, Inc., 2012, chap. 2, p. 15–39. ISBN 978-1-61324-567-5.

[36] Solymosi, K., Kövér, G. and Romvári, R. The Progression of Vegetation Indices: a Short Overview. *Acta Agraria Kaposváriensis*. april 2019, vol. 23. DOI: 10.31914/aak.2264.

[37] *Index DataBase. A Database for Remote Sensing Indices, List of Available Indices*. Available at: https://www.indexdatabase.de/db/i.php?offset=2.

[38] *NV5 Geospatial Software - Vegetation Indices*. Available at: https://www.nv5geospatialsoftware.com/docs/vegetationindices.html.

[39] Sharifi, A. Remotely sensed vegetation indices for crop nutrition mapping. *Journal of the Science of Food and Agriculture*. 2020, vol. 100, no. 14, p. 5191–5196. DOI: https://doi.org/10.1002/jsfa.10568. Available at: https://onlinelibrary.wiley.com/doi/abs/10.1002/jsfa.10568.

[40] Boiarskii, B. and Hasegawa, H. Comparison of NDVI and NDRE Indices to Detect Differences in Vegetation and Chlorophyll Content. *JOURNAL OF MECHANICS OF CONTINUA AND MATHEMATICAL SCIENCES*. november 2019, spl1. DOI: 10.26782/jmcms.spl.4/2019.11.00003.

[41] Haboudane, D., Miller, J. R., Tremblay, N., Zarco Tejada, P. J. and Dextraze, L. Integrated narrow-band vegetation indices for prediction of crop chlorophyll content for application to precision agriculture. *Remote Sensing of Environment*. 2002, vol. 81, no. 2, p. 416–426. DOI: https://doi.org/10.1016/S0034-4257(02)00018-4. ISSN 0034-4257. Available at: https://www.sciencedirect.com/science/article/pii/S0034425702000184.

[42] Schafer, R., Johnson, C., Elkins, C. and Hendrick, J. Prescription tillage: The concept and examples. *Journal of Agricultural Engineering Research*. 1985, vol. 32, no. 2, p. 123–129. DOI: https://doi.org/10.1016/0021-8634(85)90072-1. ISSN 0021-8634. Available at: https://www.sciencedirect.com/science/article/pii/0021863485900721.

[43] Robert, P. Characterization of soil conditions at the field level for soil specific management. *Geoderma*. 1993, vol. 60, no. 1, p. 57–72. DOI: https://doi.org/10.1016/0016-7061(93)90018-G. ISSN 0016-7061. Available at: https://www.sciencedirect.com/science/article/pii/001670619390018G.

[44] Sharifi, A. Using Sentinel-2 Data to Predict Nitrogen Uptake in Maize Crop. *IEEE Journal of Selected Topics in Applied Earth Observations and Remote Sensing*. 2020, vol. 13, p. 2656–2662. DOI: 10.1109/JSTARS.2020.2998638.

[45] Li, F., Li, D., Elsayed, S., Hu, Y. and Schmidhalter, U. Using optimized three-band spectral indices to assess canopy N uptake in corn and wheat. *European Journal of Agronomy*. 2021, vol. 127, p. 126286. DOI: https://doi.org/10.1016/j.eja.2021.126286. ISSN 1161-0301. Available at: https://www.sciencedirect.com/science/article/pii/S1161030121000587.

[46] Fiorio, P. R., Silva, C. A. A. C., Rizzo, R., Demattê, J. A. M., Santos Luciano, A. C. dos et al. Prediction of leaf nitrogen in sugarcane (Saccharum spp.) by vis-NIR-SWIR spectroradiometry. *HELIYON*. 2024. DOI: 10.1016/j.heliyon.2024.e26819. To appear in: HELIYON, Reference: HLY 26819.

[47] Swiss FluxNet. *Map of Flux Sites in Switzerland* [https://www.swissfluxnet.ethz.ch]. 2024. Accessed: 2024-05-02.

[48] ROTH, K. Bodenkartierung und GIS-basierte Kohlenstoffinventur von Graslandboden : Untersuchungen an den ETH-Forschungs-stationen Chamau und Fruebuel (ZG, Schweiz). *Diploma thesis, University of Zurich*. 2006. Available at: https://cir.nii.ac.jp/crid/1574231875499445376.

[49] *Thermo Fisher Scientific* [https://www.thermofisher.com/order/catalog/product/11206100]. Accessed: 2024-03-15.

[50] Frąckowiak, E., Płatek Mielczarek, A., Piwek, J. and Fic, K. Chapter Five - Advanced characterization techniques for electrochemical capacitors. In: van Eldik, R. and Hubbard, C. D., ed. *Recent Highlights II*. Academic Press, 2022, vol. 79, p. 151–207. Advances in Inorganic Chemistry. DOI: https://doi.org/10.1016/bs.adioch.2021.12.006. ISSN 0898-8838. Available at: https://www.sciencedirect.com/science/article/pii/S0898883821000477.

[51] Bréda, N. Leaf Area Index. In: Jørgensen, S. E. and Fath, B. D., ed. *Encyclopedia of Ecology*. Oxford: Academic Press, 2008, p. 2148–2154. DOI: https://doi.org/10.1016/B978-008045405-4.00849-1. ISBN 978-0-08-045405-4. Available at: https://www.sciencedirect.com/science/article/pii/B9780080454054008491.

[52] Arias, D., Calvo Alvarado, J. and Dohrenbusch, A. Calibration of LAI-2000 to estimate leaf area index (LAI) and assessment of its relationship with stand productivity in six native and introduced tree species in Costa Rica. *Forest Ecology and Management*. 2007, vol. 247, no. 1, p. 185–193. DOI: https://doi.org/10.1016/j.foreco.2007.04.039. ISSN 0378-1127. Available at: https://www.sciencedirect.com/science/article/pii/S0378112707003477.

[53] *Google Earth Engine* [Retrieved from https://earthengine.google.com/]. Accessed: 2024-04-15.

[54] R Core Team. *R: A Language and Environment for Statistical Computing*. Vienna, Austria: R Foundation for Statistical Computing, 2021. Available at: https://www.R-project.org/.

[55] Barrett, T., Dowle, M., Srinivasan, A., Gorecki, J., Chirico, M. et al. *Data.table: Extension of 'data.frame'*. 2024. R package version 1.15.99, https://Rdatatable.gitlab.io/data.table, https://github.com/Rdatatable/data.table. Available at: https://r-datatable.com.

[56] Wickham, H., François, R., Henry, L., Müller, K. and Vaughan, D. *Dplyr: A Grammar of Data Manipulation*. 2023. R package version 1.1.4, https://github.com/tidyverse/dplyr. Available at: https://dplyr.tidyverse.org.

[57] Robinson, D., Bryan, J. and Elias, J. *Fuzzyjoin: Join Tables Together on Inexact Matching*. 2020. R package version 0.1.6. Available at: https://CRAN.R-project.org/package=fuzzyjoin.

[58] Wickham, H. *Ggplot2: Elegant Graphics for Data Analysis*. Springer-Verlag New York, 2016. ISBN 978-3-319-24277-4. Available at: https://ggplot2.tidyverse.org.

[59] Kuhn and Max. Building Predictive Models in R Using the caret Package. *Journal of Statistical Software*. 2008, vol. 28, no. 5, p. 1–26. DOI: 10.18637/jss.v028.i05. Available at: https://www.jstatsoft.org/index.php/jss/article/view/v028i05.

[60] Wickham, H. *Stringr: Simple, Consistent Wrappers for Common String Operations*. 2023. R package version 1.5.1, https://github.com/tidyverse/stringr. Available at: https://stringr.tidyverse.org.

[61] Wickham, H., Vaughan, D. and Girlich, M. *Tidyr: Tidy Messy Data*. 2024. R package version 1.3.1, https://github.com/tidyverse/tidyr. Available at: https://tidyr.tidyverse.org.

[62] Irizarry, R. A. *Introduction to Data Science: Data Analysis and Prediction Algorithms with R*. 1stth ed. CRC Press, 2019.

[63] Bhandari, P. *Independent vs. Dependent Variables | Definition & Examples* [Scribbr]. February 2022. Revised on June 22, 2023. Available at: https://www.scribbr.com/methodology/independent-and-dependent-variables/.

[64] Gogtay, N. J. and Thatte, U. M. *Principles of Correlation Analysis*. 2017.

[65] Beers, B. *What Is Regression? Definition, Calculation, and Example* [Investopedia]. February 2024. Available at: https://www.investopedia.com/terms/r/regression.asp.

[66] Turney, S. *Coefficient of Determination (R^2) | Calculation & Interpretation* [Scribbr]. April 2022. Revised on June 22, 2023. Available at: https://www.scribbr.com/statistics/coefficient-of-determination/.

[67] Bobbitt, Z. *A Quick Intro to Leave-One-Out Cross-Validation (LOOCV)* [Statology]. November 2020. Posted on November 3, 2020. Available at: https://www.statology.org/leave-one-out-cross-validation/.

[68] Bobbitt, Z. *MAE vs. RMSE: Which Metric Should You Use?* [Statology]. October 2021. Posted on October 4, 2021. Available at: https://www.statology.org/mae-vs-rmse/.

[69] Nilsson, O. Winter dormancy in trees. *Current Biology*. june 2022, vol. 32, no. 12, p. R630–R634. DOI: 10.1016/j.cub.2022.04.011.

[70] Cong, Y., Zhang, Z., Liu, B., Chen, Y., Li, X. et al. Resource Remobilization Efficiency Varies With Plant Growth Form but Not Between Fens and Bogs. *Frontiers in Earth Science*. 2022, vol. 9. DOI: 10.3389/feart.2021.827721. ISSN 2296-6463. Available at: https://www.frontiersin.org/articles/10.3389/feart.2021.827721.

[71] Kozlowski, T. T. and Pallardy, S. G. CHAPTER 5 - Photosynthesis. In: Kozlowski, T. T. and Pallardy, S. G., ed. *Physiology of Woody Plants (Second Edition)*. Second Editionth ed. San Diego: Academic Press, 1997, p. 87–133. DOI: https://doi.org/10.1016/B978-012424162-6/50022-3. ISBN 978-0-12-424162-6. Available at: https://www.sciencedirect.com/science/article/pii/B9780124241626500223.

[72] Jarrell, W. and Beverly, R. The Dilution Effect in Plant Nutrition Studies. In: Brady, N., ed. Academic Press, 1981, vol. 34, p. 197–224. Advances in Agronomy. DOI: https://doi.org/10.1016/S0065-2113(08)60887-1. ISSN 0065-2113. Available at: https://www.sciencedirect.com/science/article/pii/S0065211308608871.

[73] Cui, B., Zhao, Q., Huang, W., Song, X., Ye, H. et al. A New Integrated Vegetation Index for the Estimation of Winter Wheat Leaf Chlorophyll Content. *Remote Sensing*. 2019, vol. 11, no. 8. DOI: 10.3390/rs11080974. ISSN 2072-4292. Available at: https://www.mdpi.com/2072-4292/11/8/974.

[74] Magney, T. S., Eitel, J. U. H. and Vierling, L. A. Mapping wheat nitrogen uptake from RapidEye vegetation indices. *Precision Agriculture*. august 2017, vol. 18, no. 4, p. 429–451. DOI: 10.1007/s11119-016-9463-8. ISSN 1573-1618. Available at: https://doi.org/10.1007/s11119-016-9463-8.

[75] Padilla, F. M., Peña Fleitas, M. T., Gallardo, M. and Thompson, R. B. Determination of sufficiency values of canopy reflectance vegetation indices for maximum growth and yield of cucumber. *European Journal of Agronomy*. 2017, vol. 84, p. 1–15. DOI: https://doi.org/10.1016/j.eja.2016.12.007. ISSN 1161-0301. Available at: https://www.sciencedirect.com/science/article/pii/S1161030116302519.

[76] Shanahan, J. F., Schepers, J. S., Francis, D. D., Varvel, G. E., Wilhelm, W. W. et al. Use of Remote-Sensing Imagery to Estimate Corn Grain Yield. *Agronomy Journal*. 2001, vol. 93, no. 3, p. 583–589. DOI: https://doi.org/10.2134/agronj2001.933583x. Available at: https://acsess.onlinelibrary.wiley.com/doi/abs/10.2134/agronj2001.933583x.